Science Forum (Journal of Pure and Applied Sciences)

Journal Homepage: https://atbu.edu.ng/science-forum/

Effectiveness of 3, 4 and 5- Parameters Adsorption Equilibrium Isotherm Models in Describing Arsenic Removal

AMOKO[1], J.S; FEHINTOLA[1] E.O; OJO[1], B. M; AKANNI[2] A. O; FAKOREDE[3] E.O.; FASUBA[3], A.O. and OKE[4], I.A

[1]Department of Chemistry, Adeyemi Federal University of Education, Ondo, Nigeria
[2] Civil Engineering Department, Federal Polytechnic, Ile- Oluji, Nigeria
[3] Department of Civil and Environmental Engineering, Elizade University, Ilara – Mokin, Nigeria
[4] Civil Engineering Department, Obafemi Awolowo University, Ile-Ife, Nigeria

ABSTRACT

The presence and removal of arsenic ions and salts from the environment have become worldwide environmental issues and problems because of the harmful and toxic nature of the substance. The paper presents the effectiveness of higher adsorption parameters (3, 4 and 5) in describing arsenic removal from aqueous solutions. Raw eggshells from chickens were collected from an institutional farm in Nigeria. These collected raw eggshells were washed with distilled water to remove impurities, air dried to reduce the moisture content and powdered eggshells using a silver crest blender. Energy Dispersive Spectroscopy and scanning electron microscope images of the powdered eggshell were evaluated at selected magnifications. The powdered eggshell's adsorption rates were examined in synthetic and typical arsenic-contaminated water. Parameters of adsorption equilibrium models were determined using Microsoft Excel Solver. The performances of these adsorption equilibrium models in describing arsenic removal from these arsenic-contaminated waters were evaluated statistically using the Model of Selection Criterion (MSC) and Akaike Information Criterion (AIC). The study revealed that the elemental compositions of powdered eggshells are carbon, aluminium, iron, silicon, calcium and oxygen with traces of sodium, magnesium and manganese. The mechanism of arsenic removal by adsorption using powdered eggshell includes redox and replacement reactions. Adsorption equilibrium analysis established that adsorption models' 5 and 4 parameters described the relationship between arsenic removal and the mass of the adsorbent better than the 3 and 2 parameters of adsorption models based on the values of MSC and AIC. All the 5 and 4 parameters of the adsorption models had MSC values greater than 3.0 (equivalent to greater than 0.95 correlation coefficient, 68.75 % and 17.65 % for 3 and 2 parameters of adsorption models. It was concluded that powdered eggshells removed arsenic from aqueous solutions, the removal rate was affected by the nature of the water and 5 and 4 parameters of adsorption models were effective in the description of arsenic removal by powdered eggshell.

ARTICLE INFO

Received 12 November 2023
Received in Revised Form
14 November 2023
Accepted 15 November 2023
Published 15 January 2024
Available online 15 January 2024

KEYWORDS

Arsenic,
Adsorption,
Equilibrium
Models,
Removal
Efficiency,
Higher-parameter adsorption isotherms,
Powdered eggshell

Corresponding Author: Oke, I.A ✉ okeia@oauife.edu.ng ✉ *Civil Engineering Department, Obafemi Awolowo University, Ile-Ife, Nigeria*

INTRODUCTION

Arsenic is an obvious metalloid element, which has obtained much attention due to its terrific toxicity to human health (Li et al., 2012; Yin et al., 2019; He et al., 2019). At higher arsenic concentrations exceeding the limit in the environment, long-term uptake of water, air and soil contaminating arsenic could result in neurological disorders, hypertension, diabetes, bladder cancer, and lung, liver, and kidney diseases (Yazdani et al., 2014; Yin et al, 2019). Further information, documents studies and literature on the effects of arsenic on humans and relevant organs are documented in the literature such as Arun et al. (2021); Aristizaba-Henano et al. (2021); Jin et al. (2022); Karachaliou et al. (2021); Liu et al. (2023); Babaeivelni et al. (2014); Wang et al. (2022); Tseng et al. (2021); Wakeel et al. (2020); Deliyanni et al. (2015); Koohzad et al.. (2019); Ro et al. (2022); Tu, *et al.* (2023); Wu et al. (2022); Xue et al.. (202 1); Yang et al. (2023); Yin et al. (2022); Zhou et al. (2022); Pierce and Moore (1982); Nakano et al. (2003); Osborne and Thompson (2005); Pierce and Moore (1980); Valdes et al. (2015); Tsai *et al.* (2006); Ajala et al. (2018); Guo et al. (2022); Ghosh and Sit (2015); Chen et al. (2012; 2022); Calatayud and Laparra Llopis (2015); Bailey and Fry (2015) and Calatayud et al. (2022).

Figure la shows the schematic representation of arsenic mechanisms of action within the cell. Figure 1b describes the schematic representation of routes for arsenic transport. Among the several treatment methods and technologies developed and established for the reduction of arsenic compounds and ions from the aqueous solutions and environment, adsorption treatment methods and technologies are receiving increasing consideration.

These treatment methods and technologies are becoming attractive, emerging, and promising technologies, based on vital operational factors such as simplicity and ease of operation of these treatment methods and technologies and cheaper pollution control methods. These treatment methods and technologies are easy to handle. sludge-free generation operation, and adsorbent regeneration capacity. In the engineering application of adsorption treatment methods and technologies, detailed data and information on adsorption equilibrium characters and properties are required in the design (hydraulic and process) of adsorbers. The adsorption equilibrium isotherm models provide fundamental physicochemical information and data for estimating the pertinency of the adsorption processes as unit operations. An adsorption equilibrium isotherm model or equation is a mathematical expression with parameters that express the surface characters and properties of the treatment methods and technologies. These isotherm parameters explained the affinity of the absorbent, at a fixed environmental temperature and the solution's pH. In engineering design, an accurate and exact mathematical description of the adsorption equilibrium isotherm is essential for the effective design of adsorption contact processes. Adsorption processes have been categorised based on Langmuir's classifications, types of adsorption isotherms (Al-Ghouti and Da'ana, 2020) and the number of parameters in adsorption equilibrium isotherms.

Figure 2 shows the categorisation of adsorption based on isotherm type. Figure 3 shows the categorisation of adsorption based on Langmuir's classifications. Figure 4 shows the categorisation of adsorption based on the number of parameters in adsorption equilibrium isotherms. Table 1 shows the classification of adsorption based on the number of parameters and the mathematical equations. More information and data on the adsorption treatment methods, performance and modifications, and factors that influence the performance are established in the literature such as Aber and Sheydaei (2012); Al-Ghouti and Da'ana (2020); Ayawei et *al.* (2017); Begun et al. (2016); Atallah *et al*. (2020); Dada *et al. (2021)*; Deliyanni *et al.* (2015); Feng *et al.* (2013); Guru and Dash (2014); He et al. (2012); Hee-Jeong (2019); Hee-Jong and Seung-Mok (2015) and Okafor *et al.* (2012).

The most commonly utilised materials for adsorbent are carbonaceous materials such as coconut, wood, and coal. These materials are utilised for the industrial production of activated carbons. These types of adsorbents are relatively expensive and frequently imported.

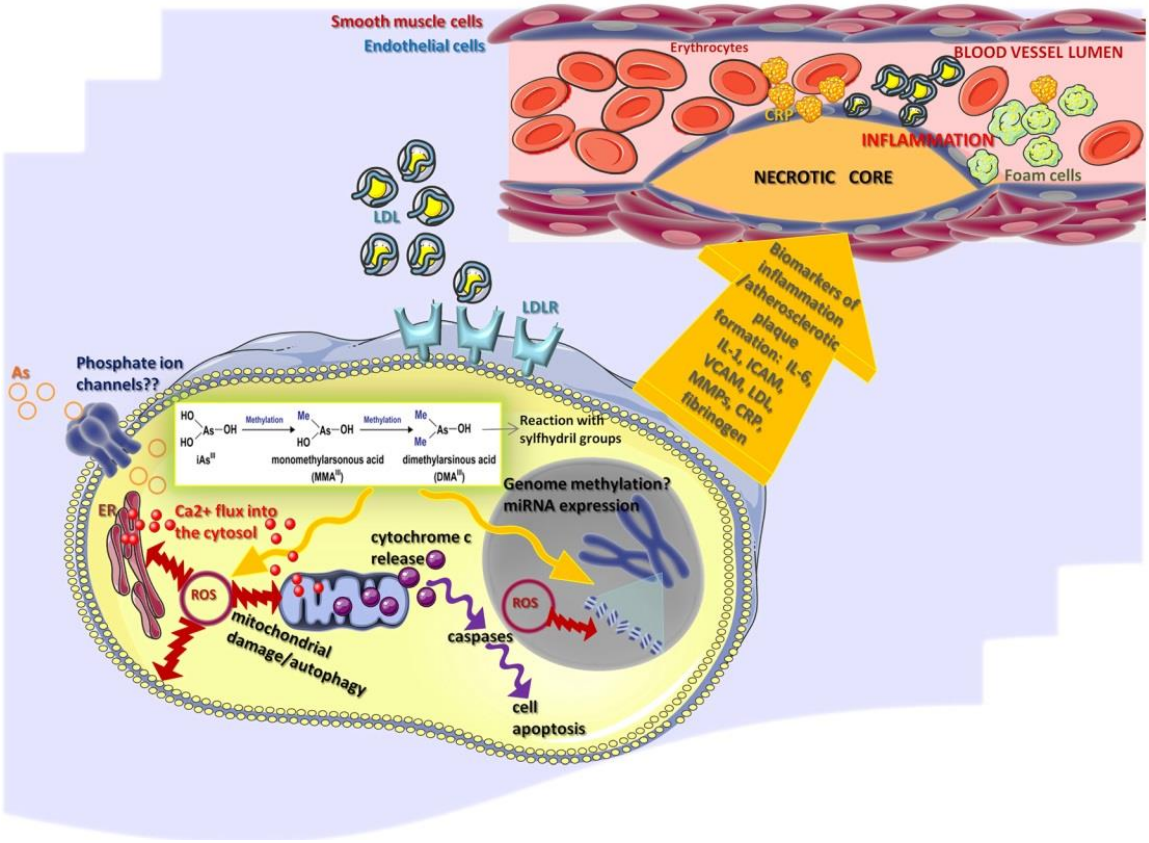

Figure 1a Schematic representation of arsenic mechanisms of action within cell (Source: Karachilou *et al.,* 2022)

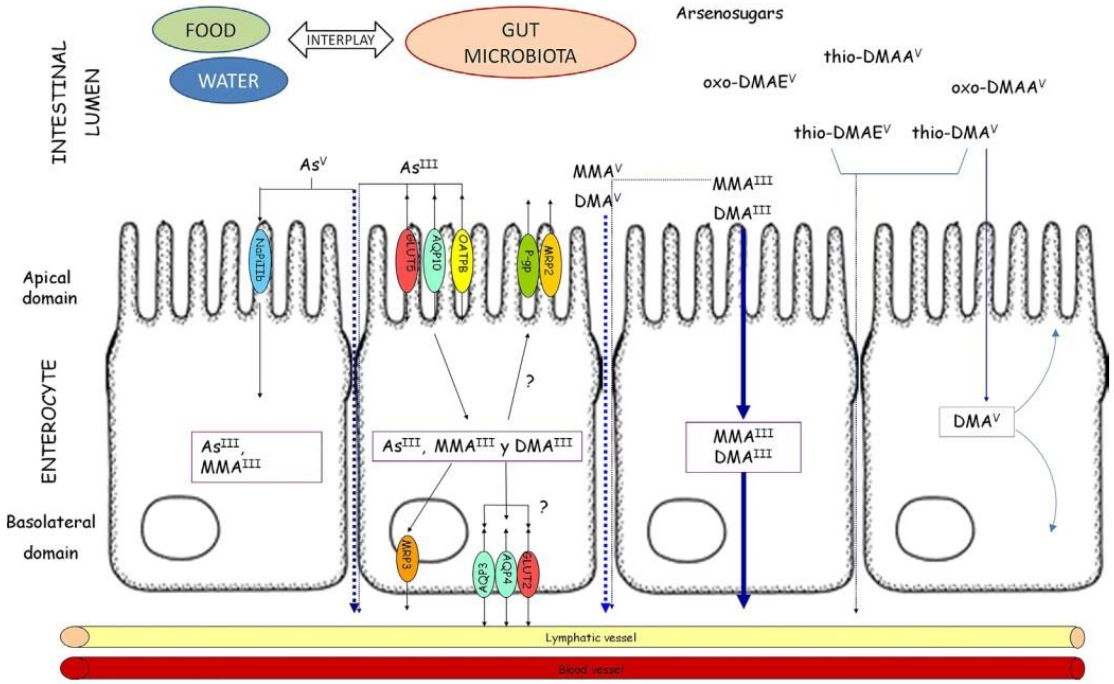

Figure 1b Schematic representation of routes for arsenic transport (Source: Calatayud and Lapara LJopis, 2015)

Isotherm type	Description	Example	Sample graph
Type I isotherms (convex upward)	Characterized by a horizontal plateau in which it maintains for very high gas pressures, and it can be described by Langmuir equation.	Adsorption of water vapor on zeolite, adsorption of hydrogen on charcoal. Iodine adsorption from potassium iodine solution on zinc chloride AC	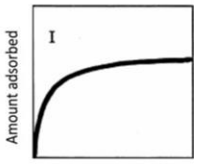
Type II isotherms	Describes adsorption on mesoporous monolayer materials at low pressure and on mesoporous multilayer material at high pressure near saturation with no hysteresis. It has one inflection point. Moreover, its observed in only microporous, nonporous, or disperse solids with > 50 nm pore diameter.	Adsorption of nitrogen on silica gel or iron catalyst, adsorption of water vapor on polymer based adsorbent	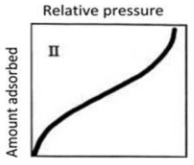
Type III isotherms (concave upward)	This type occurs where the adsorbate–adsorbate interaction is big compared to adsorbate–sorbent interaction.	Adsorption of water on hydrophobic zeolites and activated carbon, adsorption of bromine and iodine on silica gel, carbon tetrachloride adsorption on mesoporous gel	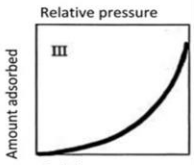
Type IV isotherms	This type describes specific mesoporous materials adsorption behavior showing the pore condensation the hysteresis which occurs between the desorption and the adsorption branch. It has 2 inflection points.	Adsorption of humid air, water vapors on specific types of activated carbon, adsorption of benzene on iron oxide and on silica gel.	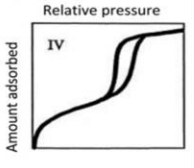
Type V isotherms	This type indicates the presence of mesopores in phase change like pore condensation could occur. It has one inflection point.	Adsorption of water on carbon molecular sieves and on activated carbon fiber.	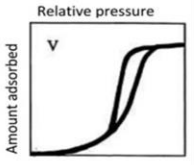
Type VI isotherms	At low temperatures, layers will become more pronounced and the isotherms presents stepwise multilayer adsorbates. It has several inflection points.	Adsorption of noble gases on the surfaces of planar graphite, and adsorption of butanol on aluminum silicate, adsorption of CH_4 on MgO	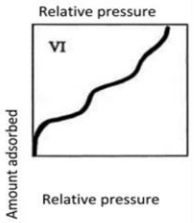

Figure 2 the categorisation of adsorption based on isotherm type. (Source: Al-Ghouti and Da'ana, 2020)

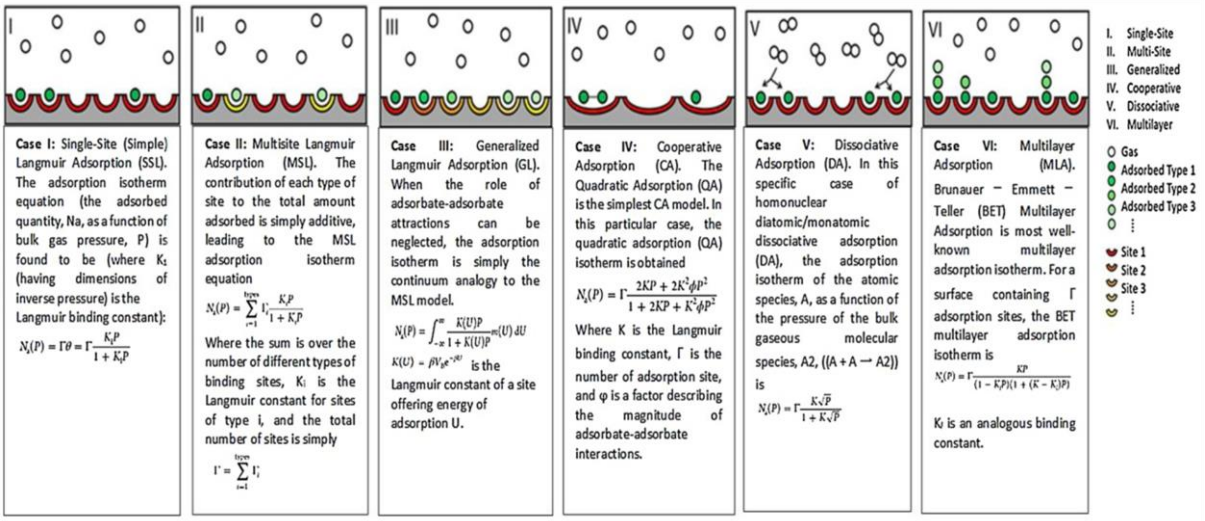

Figure 3 the categorisation of adsorption based on Langmuir's classifications. (Source: Al-Ghouti and Da'ana, 2020)

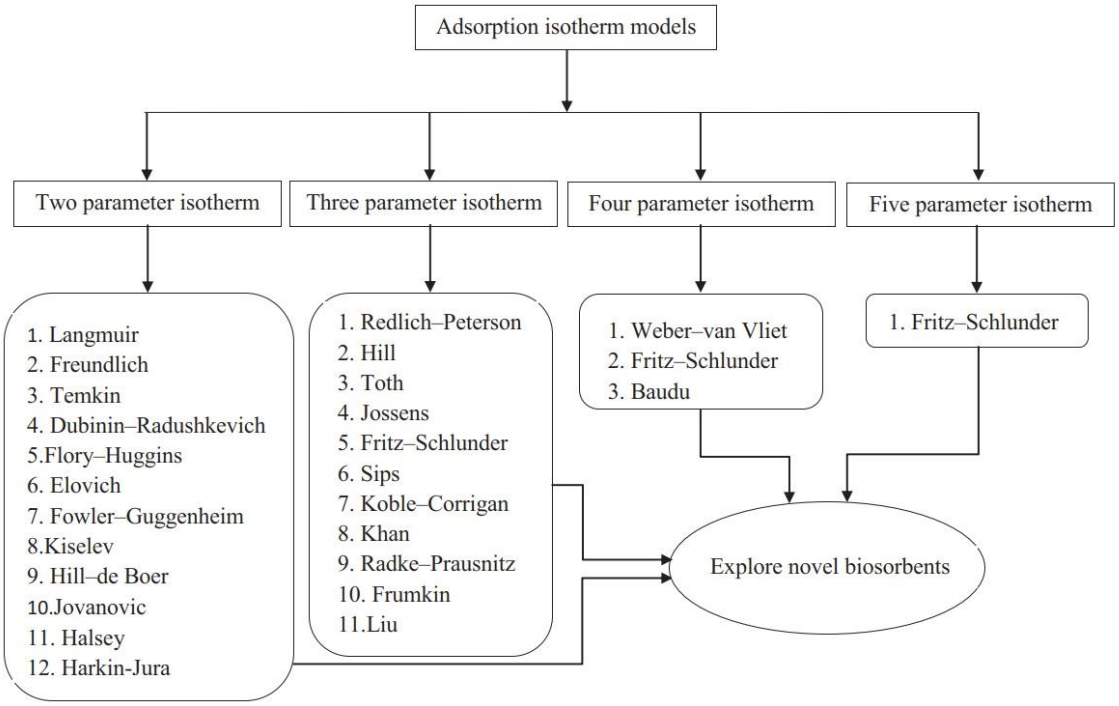

Figure 4 the categorisation of adsorption based the number of parameters in adsorption equilibrium isotherms. (Source: Al-Ghouti and Da'ana, 2020)

Table 1: the classification of adsorption based on the number of parameters and the mathematical equations for single and multi-component aqueous solutions (Sources: Hamdaoui and Naffrechoux (2007); Cano *et al.* (2007); Rangabhashiyam *et al.* (2014); Vishali and Mullai (2016); Ayawei *et al.* (2017); Al- Ghouti and Daana (2020); Outram *et al.* (2021).

Type	Name	Non- Linear Relationship	Parameters	Linear Relationship
1- Parameter	Statistical	$q_e = \left(\frac{kC_e + (kC_e)^2(\Gamma_{ii})}{1 + kC_e + (kC_e)^2\left(\frac{\Gamma_{ii}}{2}\right)} \right)$	k	
	Linear (Henry)		k_p	$q_e = K_p C_e$
2- Parameters	Langmuir	$q_e = \frac{\alpha_L \beta_L C_e}{1 + \alpha_L C_e}$	α_L and β_L	$\left(\frac{C_e}{q_e}\right) = \frac{C_e}{\beta_L} + \frac{1}{\beta_L \alpha_L}$ $\left(\frac{1}{q_e}\right) = \frac{1}{\alpha_L \beta_L C_e} + \frac{1}{\beta_L}$ $q_e = \beta_L - \frac{\beta_L q_e}{\alpha_L C_e}$ $\left(\frac{q_e}{C_e}\right) = \beta_L \alpha_L - \alpha_L q_e$ $\left(\frac{1}{C_e}\right) = \beta_L \alpha_L \frac{1}{q_e} - \alpha_L$
	Freundlich	$q_e = K_f C_e^{\frac{1}{\alpha_f}}$	K_f and α_f	$Log(q_e) = log(K_f) + \frac{1}{\alpha_f} Log(C_e)$
	Temkin	$q_e = \frac{RT}{\beta_t} \ln(\alpha_t C_e)$	α_t and β_t	$q_e = \alpha_t + 2.3\beta_t \log C_e$

Type	Name	Non- Linear Relationship	Parameters	Linear Relationship
	Dubinin–Radushkevich	$q_e = K_{dm} Exp\left(-\alpha_{dm}\varepsilon^2\right)$	K_{dm} and α_{dm}	$\ln\left(q_e\right) = \ln\left(K_{dm}\right) - \alpha_{dm}\varepsilon^2$
	Halsey A	$q_e = \left(\frac{K_H}{C_e}\right)^{\frac{1}{\alpha_H}}$	K_H and α_H	$\log\left(q_e\right) = \left(\frac{1}{N_H}\right)\log K_H - \frac{1}{N_H}\log C_e$
	Crombie-Quilty and McLoughin (1983)	$q_e = K_m\left(\frac{C_e}{M}\right)^{\frac{1}{\alpha_m}}$	K_m and α_m	$\log\left(q_e\right) = \log K_m - \frac{1}{\alpha_m}\log\left(\frac{C_e}{M}\right)$
	Frenkel- Halsey- Hill	$q_e = Exp\left(\frac{\ln\left(\left(K_{fhh}\right) - \ln\left(C_e\right)\right)}{\alpha_{fhh}}\right)$	K_{fhh} and α_{fhh}	$\ln\left(q_e\right) = \left(\frac{1}{\alpha_{fhh}}\right)\ln K_{fhh} - \frac{1}{\alpha_{fhh}}\ln C_e$
	Harkin Jura A	$q_e = \left(\frac{\left(\alpha_{hj}\right)}{\beta_{hj} + \log\left(C_e\right)}\right)^{0.5}$	α_{hj} and β_{hj}	$\log\left(q_e\right)^2 = \log\left(\alpha_{hj}\right) + \log\left(\beta_{hj} + \log C_e\right)$
	Harkin Jura B	$q_e = \left(\frac{\left(\alpha_{hj}\right)}{\beta_{hj} - \log\left(C_e\right)}\right)^{0.5}$	α_{hj} and β_{hj}	$\log\left(q_e\right)^2 = \log\left(\alpha_{hj}\right) + \log\left(\beta_{hj} - \log C_e\right)$
	Jovanovic	$q_e = K_{jm}\left(1 - \exp^{\alpha_j C_e}\right)$	K_{jm} and α_{jm}	$\log\left(q_e\right) = \log\left(K_{jm}\right) + \log\left(1 - \exp^{\alpha_j C_e}\right)$
	Elovich	$\left(\frac{q_e}{\alpha_{mE}}\right) = K_E C_e\left(\exp^{-\frac{q_e}{\alpha_{mE}}}\right)$	K_E and α_E	$\ln\left(\frac{q_e}{C_e}\right) = \ln\left(K_E\alpha_{mE}\right) - \frac{q_e}{\alpha_{mE}}$
	Folwer –Guggenhien	$K_{FG}C_e = \frac{\theta}{1-\theta}\exp\left(\frac{2\theta\alpha_{FG}}{RT}\right)$	K_{FG} and α_{FG}	$\ln\left(\frac{C_e\left(1-\theta\right)}{\theta}\right) = -\ln\left(K_{FG}\right) + \frac{2\theta\alpha_{FG}}{RT}$

Type	Name	Non- Linear Relationship	Parameters	Linear Relationship
	Hill-de Boer	$K_{Hd}C_e = \frac{\theta}{(1-\theta)}\exp\left(\frac{\theta}{(1-\theta)} - \frac{\alpha_{Hd}\theta}{RT}\right)$	K_{Hd} and α_{Hd}	$\ln\left[C_e\frac{(1-\theta)}{\theta}\right] - \frac{\theta}{(1-\theta)} = -\ln(K_{Hd}) - \frac{\alpha_{Hd}\theta}{RT}$
	Kiselev	$K_{1k}C_e = \frac{\theta}{(1-\theta)(1+\alpha_{nk}\theta)}$	K_{1k} and α_{lk}	$\frac{1}{C_e(1-\theta)} = \frac{K_{1k}}{\theta} + K_{1k}\alpha_{nk}$
	Flory - Huggins	$\frac{\theta}{C_e} = K_{FH}(1-\theta)^{N_{FH}}$; $\theta = 1 - \frac{C_e}{C_0}$	K_{FH} and α_{FH}	$\log\left[\frac{\theta}{C_e}\right] = \log(K_{FH}) + N_{FH}\log(1-\theta)$
	Langmuir - Vageler	$q_e = \left(\frac{C_f K_{LV}}{C_f + \alpha_{LV}}\right)$; $C_f = \frac{C_0 V}{m}$	α_{LV} and K_{LV}	$\log(q_e) = \log(C_f K_{LV}) - \log(C_f + \alpha_{LV})$
	Halsey B (Hamdaoui and Naffrechous, 2007)	$q_e = K_{Hf}\left(\frac{C_e}{C_0}\right)^{\frac{1}{\alpha_{Hf}}}$	K_{Hf} and α_{Hf}	$\log(q_e) = \log K_H - \frac{1}{\alpha_{Hf}}\log\left(\frac{C_e}{C_0}\right)$
	Halsey C(Rangabhashiyum *et al.*, 2014)	$q_e = \exp\left(\frac{\ln(K_{Hr}) - \ln(C_e)}{\alpha_{Hr}}\right)$	K_{Hr} and α_{Hr}	$\ln(q_e) = \frac{1}{\alpha_{Hr}}(\ln(K_{Hr}) - \ln C_e)$
3- Parameters	Redlich–Peterson	$q_e = \frac{\alpha_t C_e}{1 + \beta_t C_e^{\gamma}}$	α_t, γ and β_t	
	Sips	$q_e = \frac{\alpha_{ts} C_e^{\gamma_{ts}}}{1 + \beta_{ts} C_e^{\gamma ts}}$	α_{ts}, γ_{ts} and β_{ts}	
	Brouers-Sotolongo	$q_e = K_{BS}\left(1 - \exp\left(-\beta_{BS} C_e^{\alpha_{BS}}\right)\right)$	K_{BS}, α_{BS} and β_{BS}	

Type	Name	Non- Linear Relationship	Parameters	Linear Relationship
	Jossens	$C_e = \frac{q_e}{\beta_{jo}}\left(\exp\left(K_{jo} q_e^{\alpha_{jo}}\right)\right)$	α_{jo}, K_{jo}, and β_{jo},	
	Hill	$q_e = \frac{K_{Hi} C_e^{\alpha_{Hi}}}{\beta_{Hi} + C_e^{\alpha_{Hi}}}$	α_{Hi}, K_{Hi}, and β_{Hi},	
	Langmuir-Freundlich	$q_e = \frac{\beta_{LF} K_{LF} C_e^{\alpha_{LF}}}{1 + K_{LF} C_e^{\alpha_{LF}}}$	β_{LF}, K_{LF} and α_{LF}	
	Toth	$q_e = \frac{K_{tt} \alpha_{tt}^{\gamma_{tt}} C_e}{\left(1 + \alpha_{tt} C_e^{\gamma_{tt}}\right)^{\left(\frac{1}{\gamma_{tt}}\right)}}$	K_{tt}, $\alpha_{tt,}$ and γ_{tt}	
		$q_e = \frac{\alpha_{tt} C_e}{\left(\beta_{tt} + C_e^{\gamma_{tt}}\right)^{\left(\frac{1}{\gamma_{tt}}\right)}}$	$\alpha_{tt,}$ β_{tt} and γ_{tt}	
	Radke-Prausnitz	$\frac{1}{q_e} = \left(\frac{\alpha_{rp}}{(C_e)}\right) + \frac{\beta_{rp}}{\left(C_e^{\gamma_{rp}}\right)}$	α_{rp}, γ_{rp} and β_{rp}	
		$q_e = \frac{K_{rp} \alpha_{rp} C_e}{\left(1 + \alpha_{rp} C_e^{\gamma_{tt}}\right)}$	α_{rp}, γ_{rp} and q_{rp}	

Type	Name	Non- Linear Relationship	Parameters	Linear Relationship
	Khan	$q_e = \frac{K_k \alpha_k C_e}{\left(1+\alpha_k C_e\right)^{\gamma_k}}$	α_k, γ_k and K_k	
	Fritz and Schhunder	$q_e = \frac{K_{fs}\alpha_{fs} C_e^{\gamma_{fs}}}{\left(1+\alpha_{fs} C_e^{\gamma_{fs}}\right)}$	α_{fs}, γ_{fst} and K_{fs}	
	Frumkin	$K_{Fm}C_e = \beta_{Fm}\left(\frac{-\alpha_{Fm}\beta_{Fm}}{1-\beta_{Fm}}\right);$ $\beta_{Fm} = 1-\frac{C_e}{C_0}$	K_{Fm}, α_{Fm} and β_{Fm}	
	Koble - Corrigan	$q_e = \frac{\alpha_{kc} C_e^{\gamma_{kc}}}{\left(1+\beta_{kc} C_e^{\gamma_{kc}}\right)}$	$\alpha_{kc,}$ β_{kc} and γ_{kc}	
	Liu	$q_e = \left(\frac{K_{li}\left(C_e\beta_{li}\right)^{\frac{1}{\alpha_{li}}}}{1+\left(C_e\beta_{li}\right)^{\frac{1}{\alpha_{li}}}}\right)$	K_{li}, β_{li} and α_{li}	
	Loading ratio	$q_e = \frac{K_{Lr}\left(\beta_{Lr}C_e\right)^{\left(\frac{1}{\alpha_{Lr}}\right)}}{1+\left(\beta_{Lr}C_e\right)^{\left(\frac{1}{\alpha_{Lr}}\right)}}$	$K_{Lr,}$ β_{Lr} and α_{Lr}	
4- Parameters	Weber-Van Vliet	$C_e = K_{wvv}Q_e^{(\alpha_{wvv}\beta_{wvv}+\gamma_{wvv})}$	$K_{wvv,}$ $\alpha_{wvv,}$ β_{wvv} and γ_{wvv}	

Type	Name	Non- Linear Relationship	Parameters	Linear Relationship
	Bauder	$q_e = \left(\frac{(K_{bu})\beta_{bu} C_e^{1+\alpha_{bu}+\gamma_{bu}}}{1+\left(C_e^{1+\alpha_{bu}}\right)} \right)$	K_{bu}, β_{bu}, γ_{bu} and α_{bu} $1+ \beta_{bu},+ \alpha_{bu} <1$ And $1 + \beta_{bu},< 1$	
	Marczewsk-Jaroniec	$q_e = K_{msj}\left(\frac{\left(C_e\gamma_{msj}\right)^{\alpha_{msj}}}{1+\left(C_e\gamma_{msj}\right)^{\alpha_{msj}}} \right)^{\left(\frac{\beta_{msj}}{\alpha_{msj}}\right)}$	K_{msj}, γ_{msj}, α_{msj} and β_{msj}	
	Fritz and Schhunder	$q_e = \left(\frac{K_{FS4}\left(C_e\right)^{\alpha_{FS4}}}{1+\gamma_{FS4}\left(C_e\right)^{\beta_{FS4}}} \right)$	K_{FS4} γ_{FS4}, α_{FS4} and β_{FS4}	
5 parameters	Fritz- Schhunder	$q_e = \left(\frac{q_{fs5}\gamma_{fs5}\left(C_e\right)^{\alpha_{fs5}}}{1+K_{fs5}\left(C_e\right)^{\beta_{fs5}}} \right)$	q_{fs5}, K_{fs5}, α_{fs5} , γ_{fs5} and β_{fs5}	
Multi Component adsorption equilibrium isotherm	Langmuir, Bulter and Ockrent, Schwlb, Markham and Benton, Moriguch and Kaneniwa	$q_e = \frac{\alpha_{mLB}C_e}{1+\sum_{i=1}^{n}\beta_{mLB}C_{ei}}$	α_{mLB} and β_{mLB}	
	Fritz and Schhunder	$q_e = \frac{\alpha_{mFS}C_e^{\gamma_{mFS}}}{\left(\beta_{mFS}+\sum_{i=1}^{n}\alpha_{mFS}C_{ei}^{\gamma_{mFS}}\right)}$	α_{mFS}; β_{mFS} and γ_{mFS}	
	Yon and Turnock	$q_e = \frac{\alpha_{mTY}\left(C_e\right)^{\gamma_{mTY}}}{1+\sum_{i=1}^{n}\beta_{mTY_i}\left(C_e\right)^{\gamma_{mTY}}}$	α_{mFS}; β_{mFS} and γ_{mFS}	

Type	Name	Non- Linear Relationship	Parameters	Linear Relationship
Multi Component adsorption equilibrium isotherm	Redlich–Peterson	$q_e = \frac{\alpha_{mLRP} C_{ei}}{1+\sum_{i=1}^{n} \beta_{mLRP} C_{ei}}$	α_{mLRP} and β_{mLRP}	
	Ruthven	$q_e = \left(\frac{K_{mRu} \left(C_e\right)^{\alpha_{mRu}}}{1+\sum_{j=1}^{n} K_{mRuj} \left(C_e\right)^{\gamma_{mRuj}}} \right)$	K_{mRu}; α_{mRu} and γ_{mRu}	
	Sheindorf et al. (1983),	$q_e = K_{si}\left(C_{ei}\right)\left(\sum_{j=1}^{n} K_{sij} C_{ej} \right)^{(\alpha_{si}-1)}$	K_{si} and α_{si}	
	Ruthven and Wong	$q_e = \frac{K_{RWi} C_{ei} \left(1+\sum_{j=1}^{n} K_{RWj} C_{ej} \Gamma_j \right)}{1+\sum_{k=1}^{n} K_{RWk} C_{ek} \left(1+\sum_{j=1}^{n} K_{RWj} C_{ej} \frac{\Gamma_j}{2} \right)}$	K_{si} and α_{si}	
	Jain and Snoeyink	$q_{e2} = \left(\frac{\left(K_{mjs2}\right) \beta_{mjs2} C_{e2}}{1+\beta_{mjs1} C_{e1} + \beta_{mjs2} C_{e2}} \right)$ $q_{e1} = \left(\left(\frac{\left(K_{mjs1} - K_{mjs2}\right) \beta_{mjs1} C_{e1}}{1+\beta_{mjs1} C_{e1}} \right) - \left(\frac{\left(K_{mjs2}\right) \beta_{mjs2} C_{e2}}{1+\beta_{mjs1} C_{e1} + \beta_{mjs2} C_{e2}} \right) \right)$	Kmjs2; Kmjs1; β_{mjs1} and β_{mjs2}	

Type	Name	Non- Linear Relationship	Parameters	Linear Relationship
Multi Component adsorption equilibrium isotherm	Extended Langmuir	$q_{e2} = \left(\frac{\left(K_{mel2}\right)\beta_{mel2}C_{e2}}{1+\beta_{mel1}C_{e1}+\beta_{mel2}C_{e2}}\right)$ $q_{e1} = \left(\left(\frac{\left(K_{mel1}\right)\beta_{mel1}C_{e1}}{1+\beta_{mel1}C_{e1}+\beta_{mel2}C_{e2}}\right)\right)$	$K_{mel2;}$ K_{mel1}; β_{mel1} and β_{mel2}	
	Extended Langmuir - Freundlich	$q_{e2} = \left(\frac{\left(K_{melf2}\right)\left(\beta_{melf2}C_{e2}\right)^{\gamma_{melf2}}}{1+\left(\beta_{mel1}C_{e1}\right)^{\gamma_{melf1}}+\left(\beta_{mel2}C_{e2}\right)^{\gamma_{melf2}}}\right)$ $q_{e1} = \left(\left(\frac{\left(K_{melf1}\right)\left(\beta_{melf1}C_{e1}\right)^{\gamma_{melf1}}}{1+\left(\beta_{melf1}C_{e1}\right)^{\gamma_{melf1}}+\left(\beta_{melf2}C_{e2}\right)^{\gamma_{melf2}}}\right)\right)$	K_{melf2}; γ_{melf1} K_{melf1}; β_{melf1} γ_{melf2} and β_{melf2}	
	Extended Jovanovic - Freundlich	$q_{e2} = \left(\left(\frac{\left(K_{mejf2}\right)\beta_{mejf2}C_{e2}}{\beta_{mejf1}C_{e1}+\beta_{mejf2}C_{e2}}\right)\times\left[1-\exp^{-\left(\beta_{mejf1}C_{e1}+\beta_{mejf2}C_{e2}\right)^{\overline{\gamma_{mejf}}}}\right]\right)$ $q_{e1} = \left(\left(\frac{\left(K_{mejf1}\right)\beta_{mejf1}C_{e1}}{1+\beta_{mejf1}C_{e1}+\beta_{mejf2}C_{e2}}\right)\times\left[1-\exp^{-\left(\beta_{mejf1}C_{e1}+\beta_{mejf2}C_{e2}\right)^{\overline{\gamma_{mejf}}}}\right]\right)$	K_{mejf2}; γ_{mejf1} K_{mejf1}; β_{mejf1} γ_{mejf2} and β_{mejf2}	
	Single Component Jovanovic - Freundlich	$q_e = K_{scjf}\left[1-\exp^{-\left(\beta_{scjf}C_e\right)^{\gamma_{scjf}}}\right]$	K_{scjf}; β_{scjf} and γ_{scjf}	

These factors of relatively expensive and frequently imported make it important and necessary for developing and developed countries to discover cheaper, economical and available raw materials for the preparation and development of activated carbon for utilization in industries, purification of drinking water from both groundwater and surface water sources and wastewater treatment. In an attempt to produce cheaper and inexpensive activated carbon, various studies have been conducted on the biodegradable part or fraction of solid products, solid wastes, and solid residues from agricultural products (such as vegetables and animal substances), forestry, and solid wastes from related industries (such as industrial solid wastes and municipal solid waste). Bio-adsorption treatment methods and technologies are biological methods of environmental pollution control, which are alternative technologies to conventional wastewater treatment facilities. Other suitable agricultural waste products such as olive-waste cakes, cattle-manure compost, chicken eggshells; bamboo materials, coconut shells and apple pulp have been examined and evaluated as adsorbents in recent years as activated carbon precursors.

Figure 5 presents information on the performance of adsorption in terms of pollutants, adsorbents relevant adsorption equilibrium isotherms and sources. More information on the techniques and methods for arsenic reduction removal are well documented in the literature such as Alka *et al.* (2020); Amen *et al.* (2020); An *et al.* (2011); Analia *et al.* (2019); Babaeivelni *et al.* (2014); Bentahar *et al.* (2016); Daus *et al.* (2004); Hamayun *et al.* (2014); He *et al.* (2012); Koohzad *et al.* (2019); Kumar *et al.* (2004); Kundu and Gupta (2006); Li *et al.* (2014); Lin *et al.* (2006); Lopez-Luna *et al.* (2019); Manna and Ghosh (2007); Matusik (2014); Min *et al.* (2015); Mukhopaahyay *et al.* (2017); Namasivayam and Sendthikumar (1998); Obijole *et al.* (2022); Oke *et al.* (2022a and b); Oke *et al.* (2008); Ramesh *et al.* (2007); Sahabi *et al.* (2009); Shakoor *et al.* (2018); Shih (2005); Singh and Pant (2004) and Khanam *et al.* (2019). In addition, information and established mechanisms of arsenic adsorption for the environment can be established in relevant and recent literature such as Zubair *et al.* (2020); Pandi *et al.* (2020); He *et al.* (2019); Yin *et al.* (2019); Zhou *et al.* (2019); Fan *et al.* (2020); Zhu and Yan (2016); Zhu *et al.* (2018); Hu *et al.* (2017); Park *et al.* (2016); Santra and Sarkar (2016); Zhu *et al.* (2016); Zhu *et al.* (2015); Wang *et al.* (2016); Liu *et al.* (2015); Zhang *et al.* (2017); Lorenzen *et al.* (2018); Li *et al.* (2012) and Malana *et al.* (2011). Atallah *et al.* (2020) reported that the comparison between 2-parameters, 3- parameters, and 5-parameters of adsorption models revealed that the models with higher parameters were more suitable to define the equilibrium data than the adsorption models with lower parameters, but utilizations of these higher parameters' models are rare or not available in the literature. The main objectives of this research work are to utilise higher parameters (3, 4 and 5 parameters) adsorption models to explain adsorption equilibrium data of arsenic reduction and removal from both synthetic and natural water and evaluate the accuracy of selected models statistically.

MATERIALS AND METHODS

Powdered eggshell was prepared from raw and unprocessed chicken eggshells collected from an institutional agricultural farm at Obafemi Awolowo University. The preparation processes are as detailed in previous studies such as Obijole *et al. (*2022); Oke *et al*. (2022a; 2022b, 2008); Adekunbi *et al*. (2019; 2023*);* and Babajide *et al. (*2022). Figure 6 presents a summary of the powdered eggshell preparation processes. The structural characteristics of the powdered eggshells were investigated by characterization with a Scanning Electron Microscope (model Carl Zeiss Smart Evo 10) with the aid of Energy Dispersive Spectroscopy. These prepared powdered eggshells of different sizes were utilised as adsorbents for arsenic removal or reduction from both typical and synthetic wastewater.

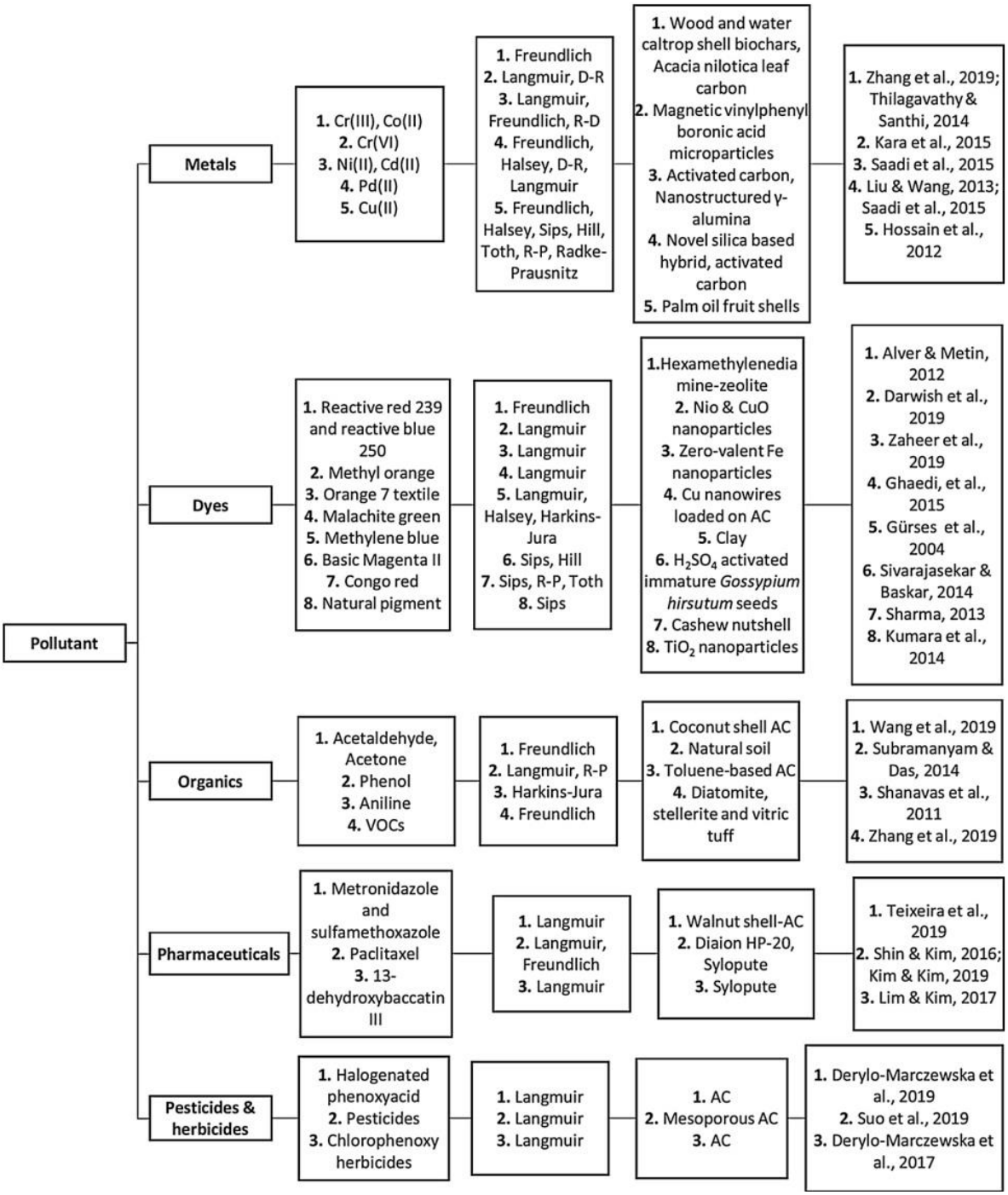

Figure 5: Information on the performance of adsorption in terms of pollutants, adsorbents relevant adsorption equilibrium isotherms and sources (Source: Al-Ghouti and Da'ana, 2020)

Evaluation of adsorption performances of the powdered eggshell was conducted utilising procedures and steps highlighted in the literature such as Obijole *et al. (*2022); Oke *et al*. (2022a; 2022b, 2008); Adekunbi *et al. (*2019; 2023*);* and Babajide *et al. (*2022). In the case of adsorptive rates of powdered eggshell for natural and typical water samples, raw water samples from Aponmu River, which is an artificial lake in Elizade University, Ilara – Mokin were utilised. Raw water samples were collected weekly for four months, a specific mass (10 grams of Sodium arsenate ($Na_2HAsO_4.7H_2O$, 99% purity) of arsenic from the stock solution was introduced (added) and the working concentrations were subjected to similar treatments as the synthetic wastewaters. The adsorption equilibrium

isotherms were calculated as follows (equation 1):

$$q_e = \left(\frac{C_0 - C_e}{M}\right)V \quad (1)$$

Where: q_e is the adsorption capacity of the powdered eggshell at equilibrium (mg/g), C_0 is initial the concentration of arsenic in the solution (mg/l), C_e is the experimental concentration of arsenic in the solution at equilibrium (mg/l), M is the mass or weight of adsorbent used (g) and V is the volume of an aqueous solution of arsenic used. The initial and final concentrations of arsenic in both untreated and treated water of both synthetic and typical water samples were determined using procedures as stated in Standard Methods (APHA, 2012; van Loosdrecht *et al.,* 2016). The adsorption equilibrium isotherm parameters in the higher parameter's models (mainly 3, 4 and 5–parameters) were calculated utilising iteration technique through Microsoft Excel Solver. Microsoft Excel Solver was utilised for the calculation of the standard adsorption equilibrium isotherm's variables based on accessibility and accuracy at no additional installation and operational costs. Figure 7 shows the Flowchart of the methodology used in the evaluation of the adsorption capacities of powdered eggshells. Figure 8 presents the flowchart of utilising Microsoft Excel Solver in the computation of the adsorption equilibrium isotherm's parameters. These calculated adsorption equilibrium parameters were utilised to compute adsorption capacity and the calculated adsorption capacities were evaluated using standard statistical methods (Analysis of Variation, Model of Selection Criterion, and Akaike Information Criterion). Information and techniques on the computations of standard statistical methods are documented in the literature such as Ojo *et al. (2023);* Obijole *et al. (*2022); Oke *et al.* (2022a; 2022b, 2008); Adekunbi *et al*. (2019; 2023); Babajide *et al. (2022);* and Fajobi *et al.* (2023).

RESULTS AND DISCUSSION

Figures 9a, 9b and 9c present the scanning electron microscope views and micrographs of the pore variations and surface morphology of the powdered eggshell as an adsorbent before the adsorption process. These figures revealed that the surface of the applied powdered eggshell was porous with a large number of continuous and discontinuous pores as functions or forms of megapores and micropores, which makes it appropriate for the adsorption of arsenic from the aqueous solutions

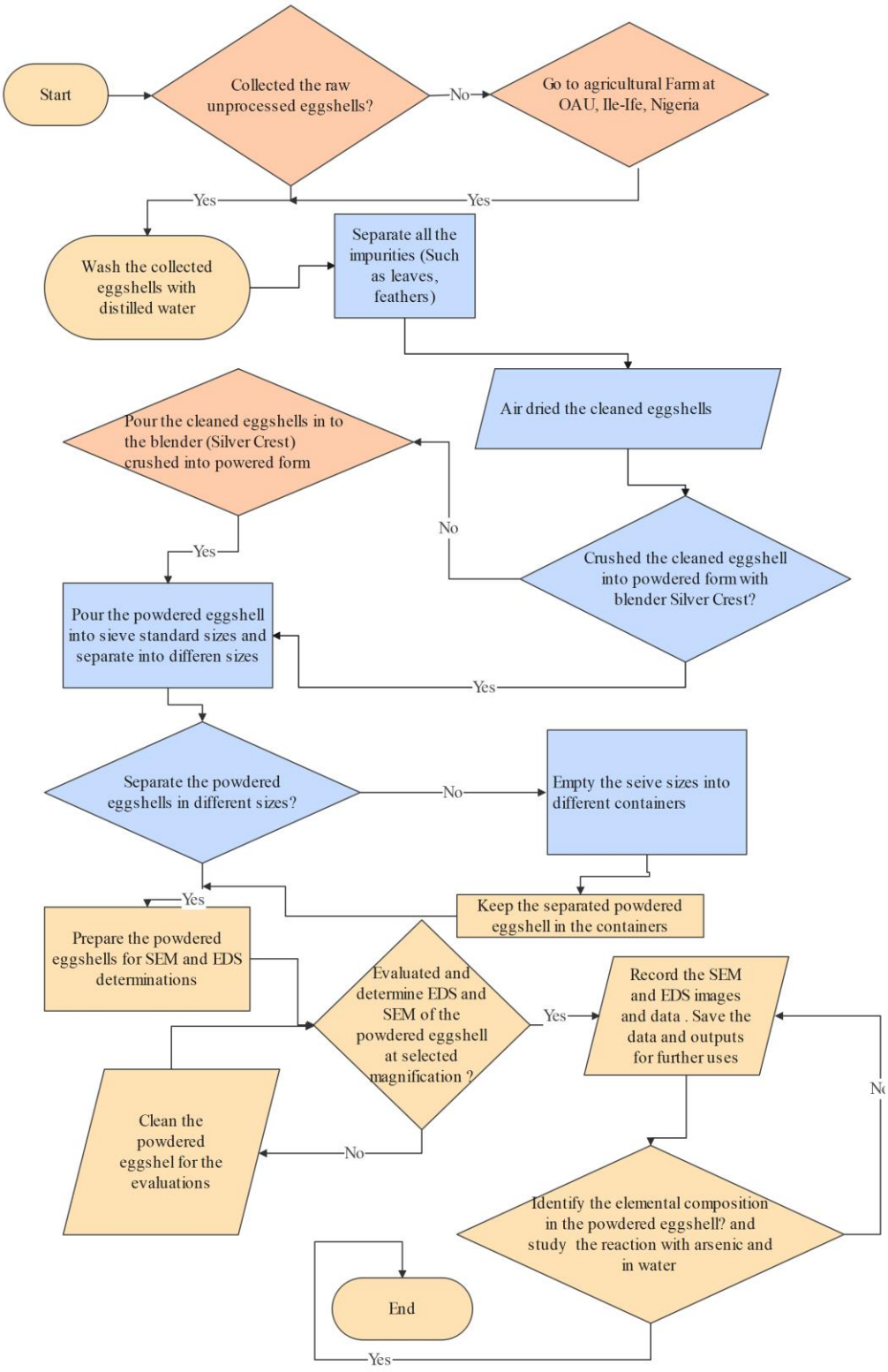

Figure 6 the summary of the powdered eggshell preparation processes and a flowchart of the methodology utilised in this study

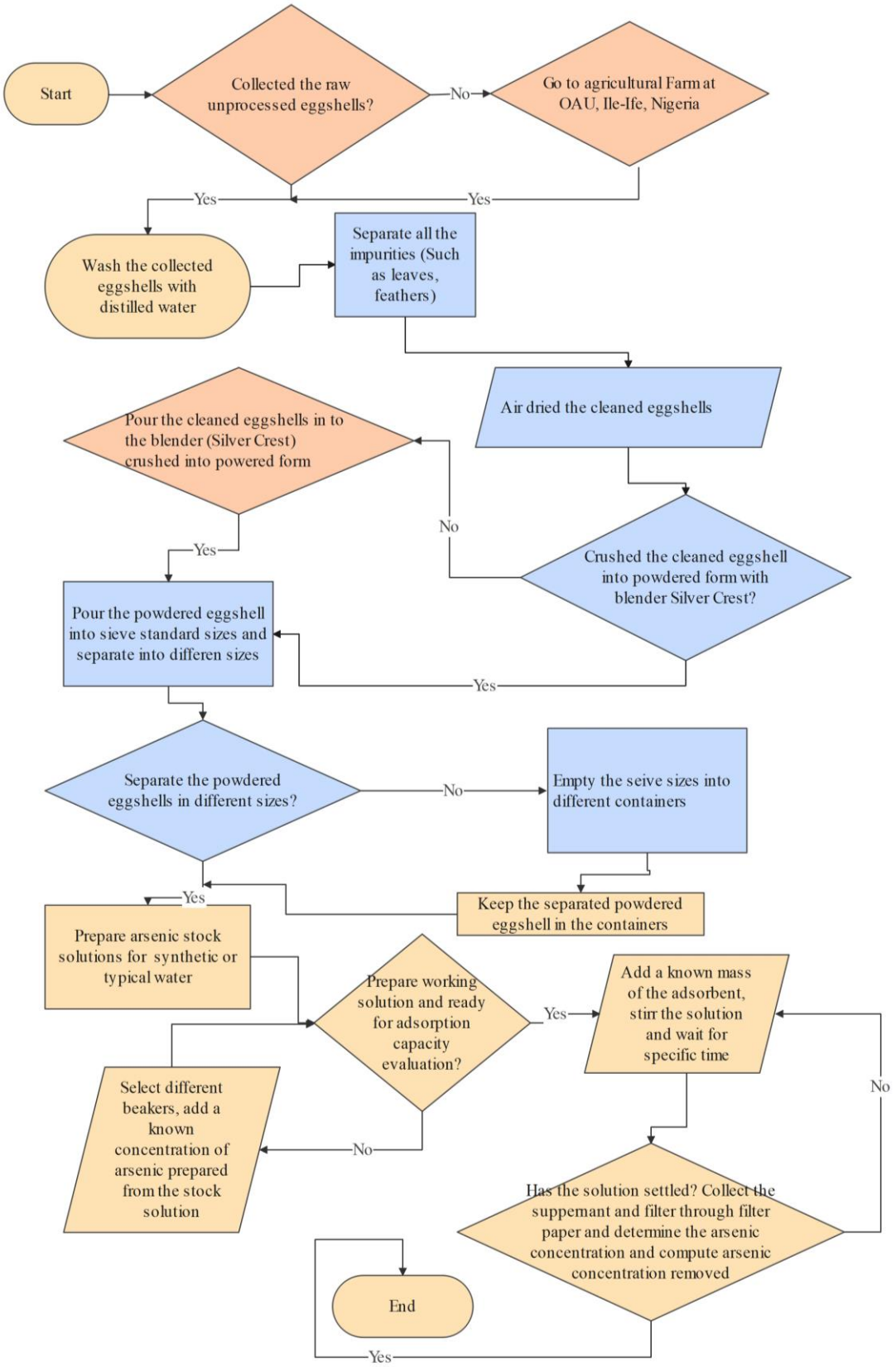

Figure 7 Flowchart of the methodology used in the evaluation of the adsorption capacities of powdered eggshell

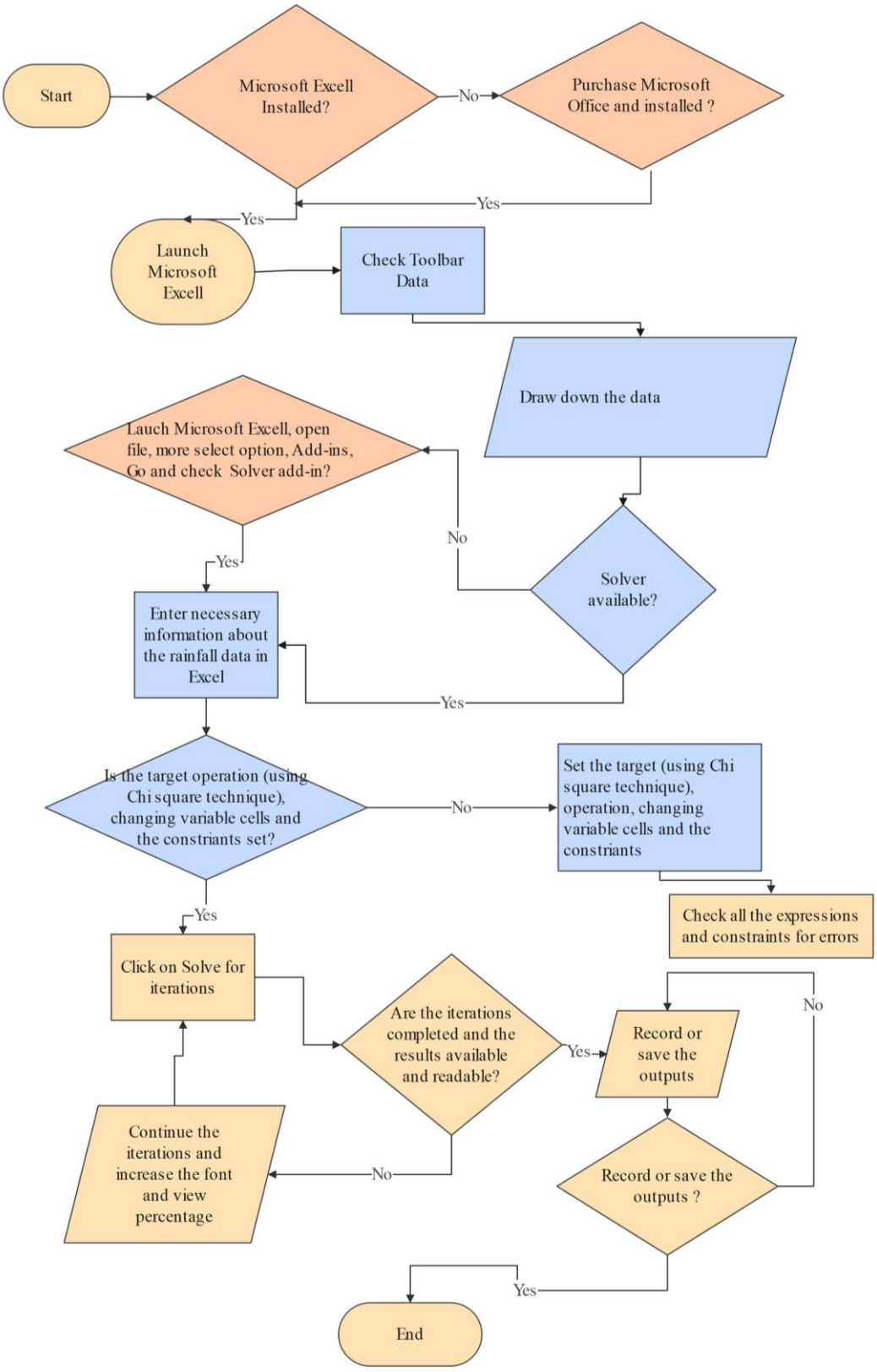

Figure 8 Flowchart of the methodology of utilizing Microsoft Excel Solver

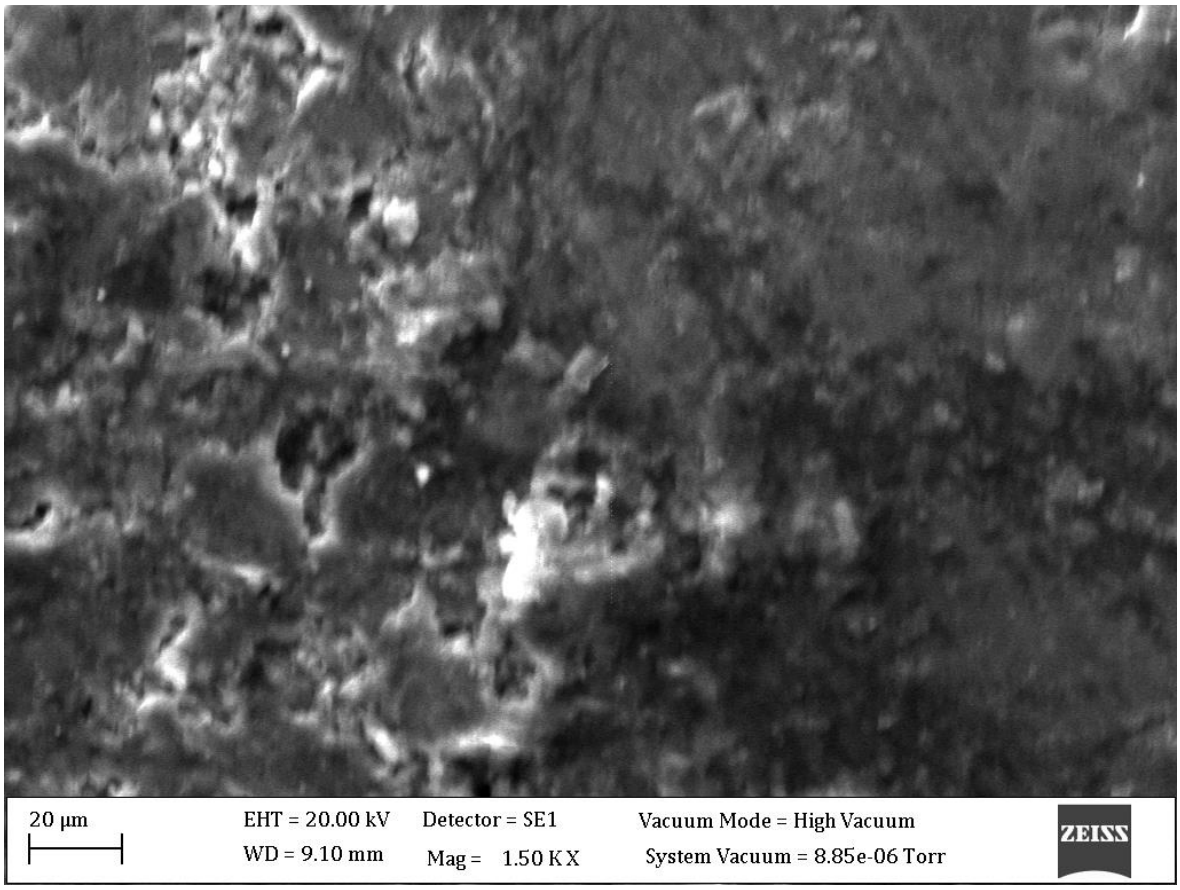

Figure 9a Surface morphology of the powdered eggshell at system vacuum of 8.85 x 10^{-6} Torr and 1500 X magnification

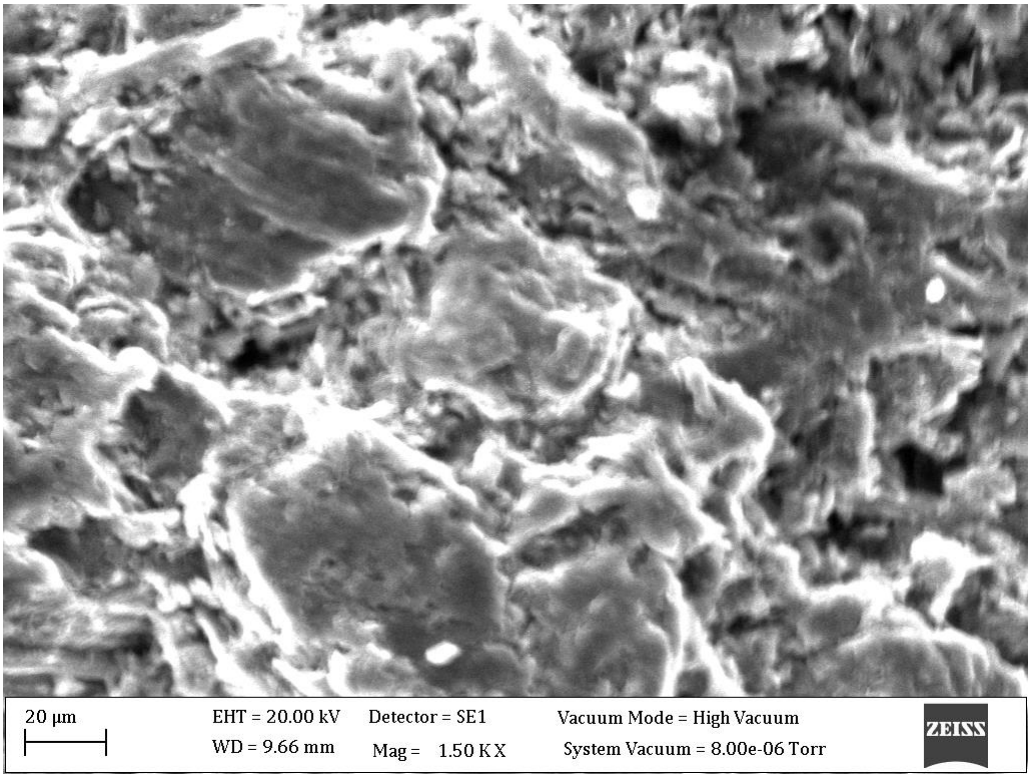

Figure 9b Surface morphology of the powdered eggshell at system vacuum of 8.00 x 10^{-6} Torr and 1500 X magnification

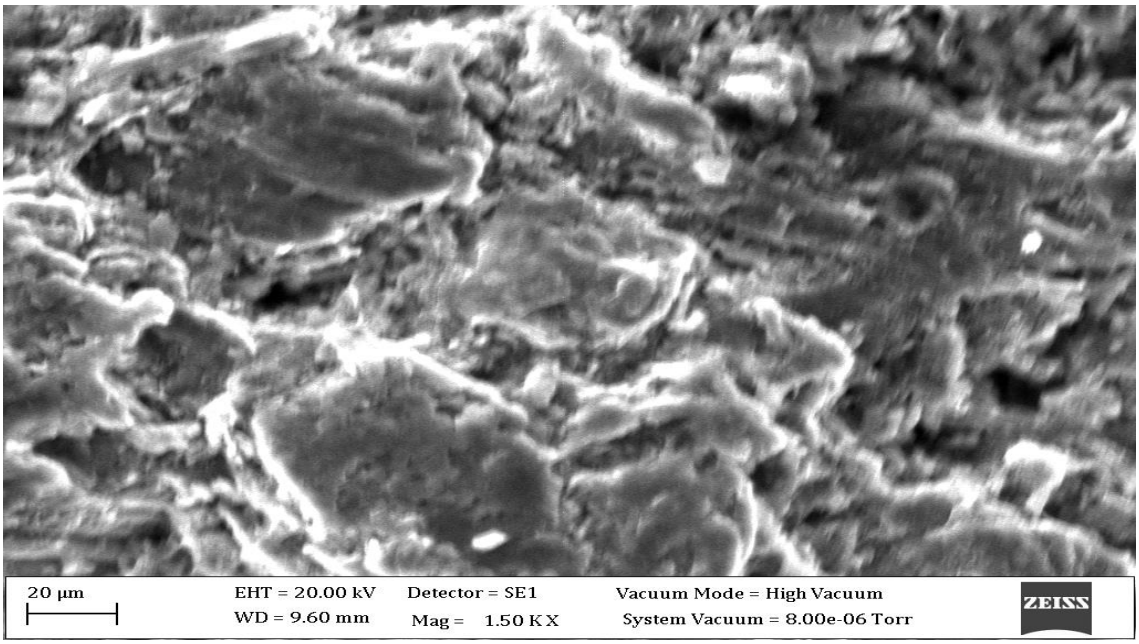

Figure 9c Surface morphology of the powdered eggshell at system vacuum of 8.85 x 10^{-6} Torr and 1500 X magnification

Figures 9a, 9b and 9c provide an outline of the microstructural geomorphology of the powdered eggshell. These four figures at different magnifications provide information and data on the mixed segregation and homogeneity of the micro compositions and constituents. In these figures, there is a fair distribution of constituents with a marked absence of several segregation. In the case of the higher magnification micrograph there are smaller regions of accumulation. These regions were tended to form clumps with the border and the pore structure is apparent.

The pores are permeate and evenly sized throughout the entire structure. In addition, these pores serve to encompass the surface area of the powdered eggshell and aid in the adsorption of impurities. Figure 10 exhibits the Scanning Electron Microscope pictures of the eggshell with other materials. These figures showed the presence of particles agglomerates with irregular shapes. In addition, these particles present clearly higher surface and certainly higher porosity than eggshell particles in accordance with the results literature. From previous studies such as Elkady et al. (2011); Köse and Kıvanç (2011); Cheng et al. (2011); Chen et al. (2012); Polat and Aslan (2014); Guru and Dash (2014); Aslan et al. (2015); . Hee-Jeong and Seung-Mok (2015), Elabbas et al. (2016); Zhang et al. (2017); Choi (2019a and b); Yusuff (2019); Candido et al. (2019); Hee-Jong (2019); Kohzad *et al.* (2019) and Rápó et al. (2020) reported some similar observations of pores for selected absorbents in the removal of arsenic. These results of microstructural geomorphology agreed with previous studies and research works.

Figures 10a, 10b, and 10c present the sscanning electron microscope images and micrographs, and Energy Dispersive Spectroscopy results of selected adsorbents used for arsenic reductions and removal from previous studies. Figure 11 presents the results of the Energy Dispersive Spectroscopy. These figures (Figures 11a, and 11b) revealed the major composition of the powdered eggshells. The major elemental components of the powdered eggshells are aluminium (between 1.25 and 7.58 % of the adsorbent as aluminium), Calcium (between 3.7 and 10.12% of the adsorbent as calcium), Silicon (between 11.15 and 25.62 % of the adsorbent as silicon), Carbon (between 0.00 and 27.75% of the adsorbent as carbon) and oxygen (between 48.75and 58.13% of the adsorbent as oxygen) had the highest weight percentages (Figure 10a, and 10b).

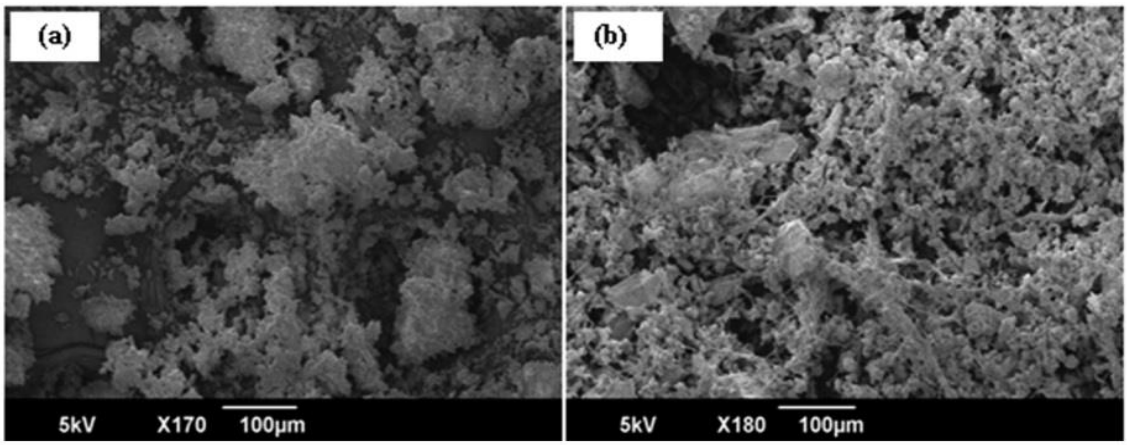

Figure 10a: scanning electron microscope images of eggshell (a) and powdered marble (b) at 100 x 10^{-6} m (Source: Elabbas et al., 2015)

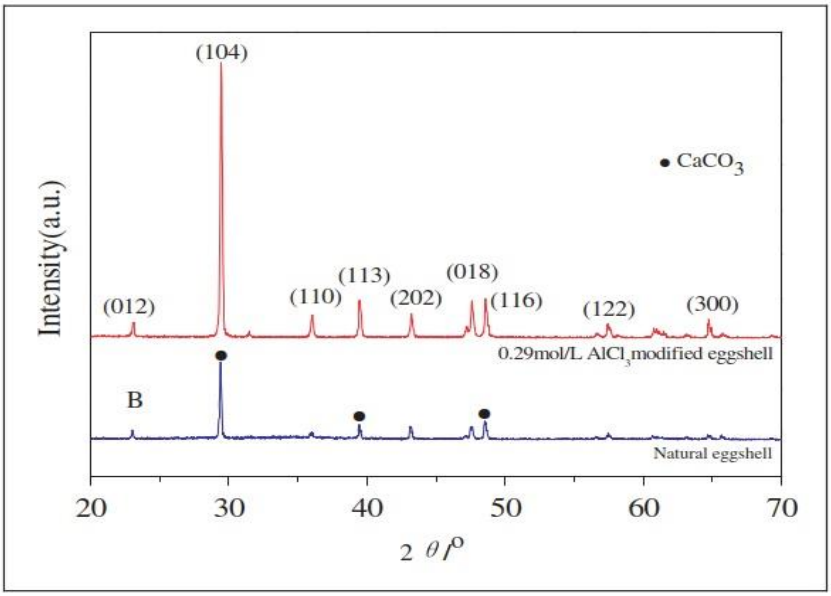

Figure 10b X-ray diffiraction spectra of natural eggshell and Al-eggshell (Source: Zhang et al 2017)

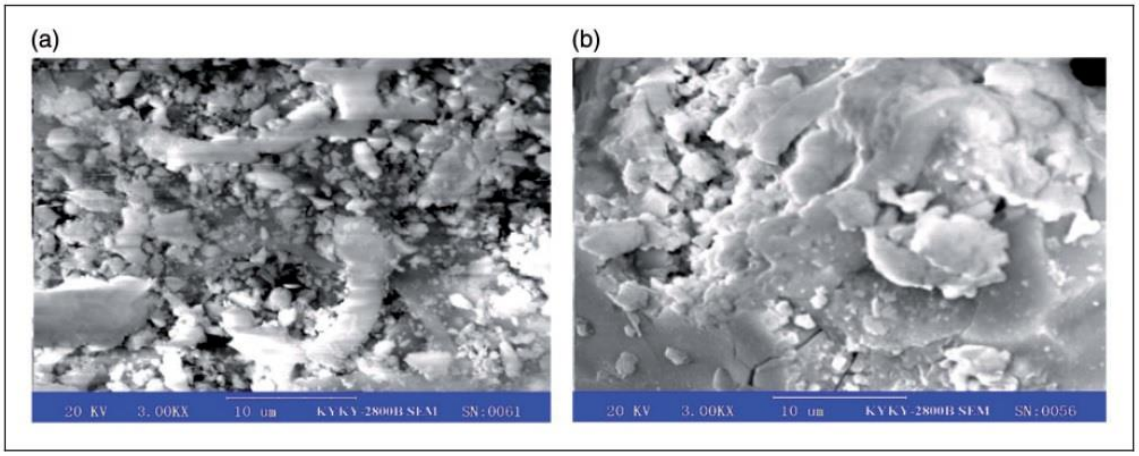

Figure 10c Scanning Electron Microscope images of natural eggshell (Label (a)) and Al-eggshell (Label (b)). (Source: Zhang et al., 2017)

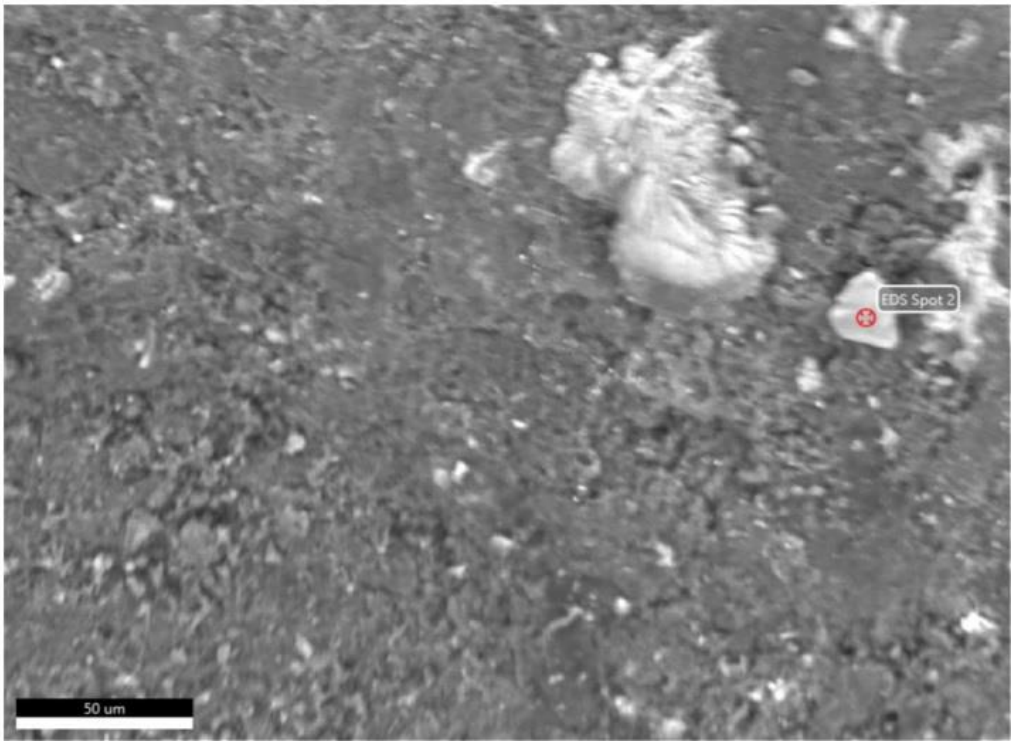

Figure 11ai: Energy Dispersive Spectroscopy view of Spot 2

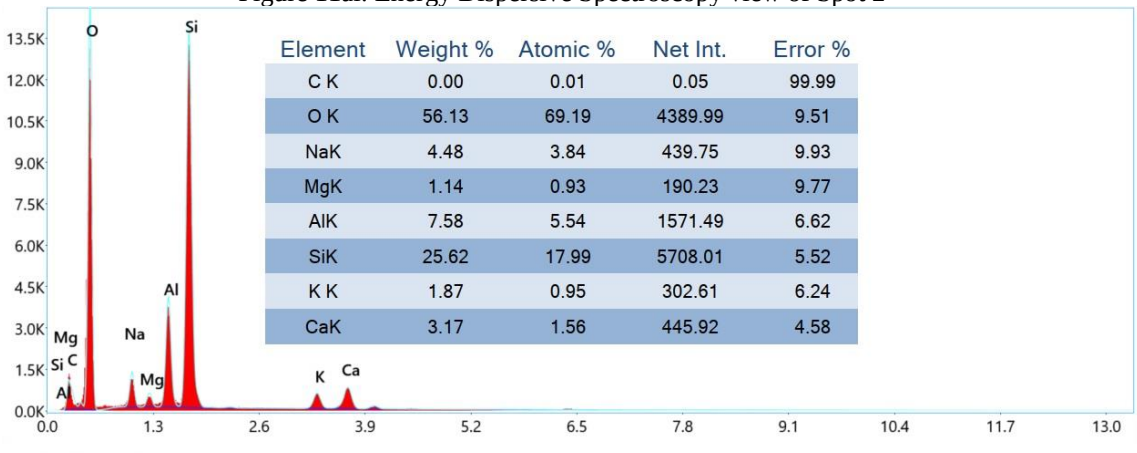

Element	Weight %	Atomic %	Net Int.	Error %
C K	0.00	0.01	0.05	99.99
O K	56.13	69.19	4389.99	9.51
NaK	4.48	3.84	439.75	9.93
MgK	1.14	0.93	190.23	9.77
AlK	7.58	5.54	1571.49	6.62
SiK	25.62	17.99	5708.01	5.52
K K	1.87	0.95	302.61	6.24
CaK	3.17	1.56	445.92	4.58

Figure 11aii: Energy Dispersive Spectroscopy results of Spot 2

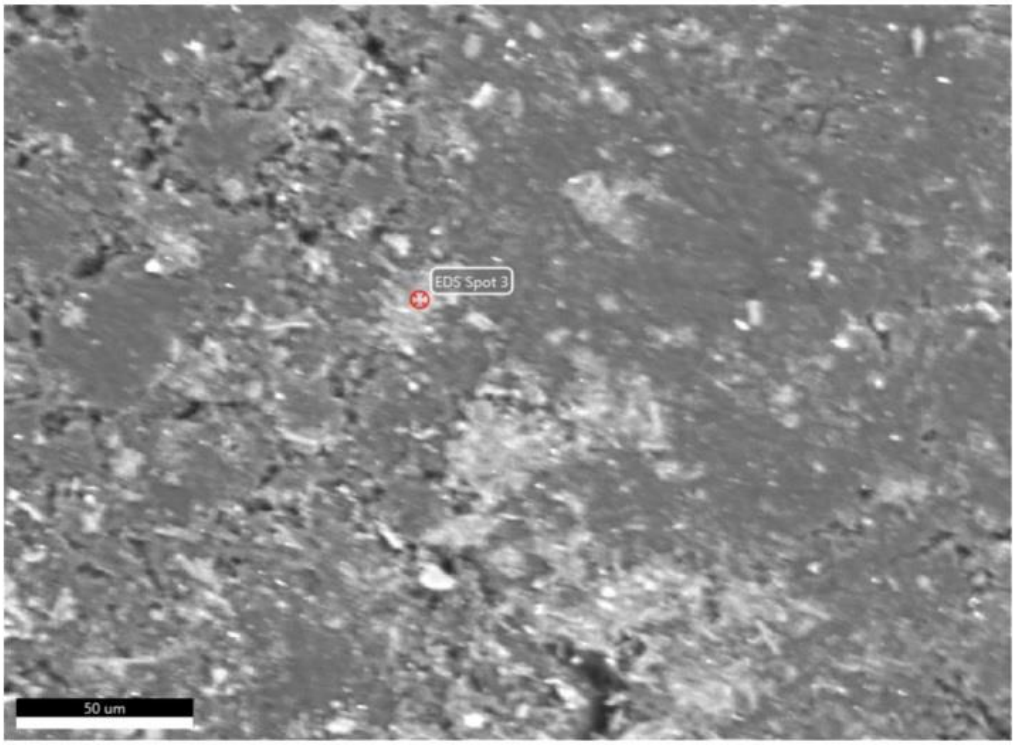

Figure 11bi: Energy Dispersive Spectroscopy view of Spot 3

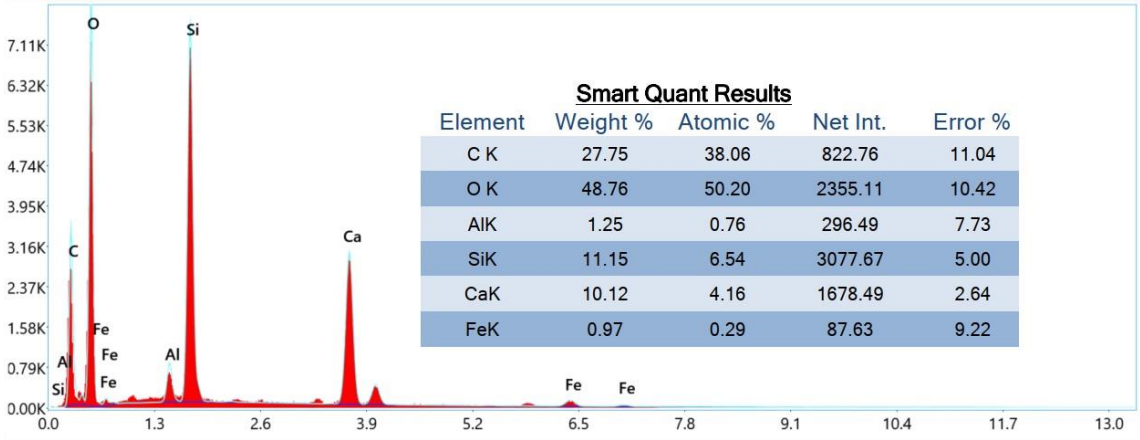

Smart Quant Results

Element	Weight %	Atomic %	Net Int.	Error %
C K	27.75	38.06	822.76	11.04
O K	48.76	50.20	2355.11	10.42
AlK	1.25	0.76	296.49	7.73
SiK	11.15	6.54	3077.67	5.00
CaK	10.12	4.16	1678.49	2.64
FeK	0.97	0.29	87.63	9.22

Figure 11bii Energy Dispersive Spectroscopy results of Spot 3

The other elements present in the adsorbent structure were Na, Mg, K, and Fe and their corresponding weight and atomic percentages are presented in the figures. The figures revealed that elemental compositions of eggshells are similar but with different proportions. These results of elemental compositions, agreed with Guru and Dash (2014) statement and composition which stated that the eggshells are composed of nearly 95% of calcium carbonate (Calcium, Carbon and Oxygen) in the form of calcite and almost 3.5 % of proteins, proteoglycans and glycoproteins. The exact and main role played by the organic components of the eggshell in the adsorption is fairly understood as in the formation of functional groups. In addition, Ajala et al. (2018) reported that elemental concentrations obtained from eggshells were: calcium 2300.33 mg/L as calcium, magnesium 850.00 mg/L as magnesium, sodium 33.83 mg/L of sodium, potassium 17.06 mg/L as potassium; iron 1.4 mg/L of iron, zinc 0.99 mg/L as zinc and copper 0.063 mg/L as copper. The proximate showed that the other components of powdered eggshells are as follows moisture content 0.95 %, ash content 45.29 % , crude protein 1.40 %, lipid content 0.37 %, lipid; 4.38 % and crude fibre 0.32 %.

Rapo et al. (2020) Due to their porous structure, eggshells have large specific surface areas; therefore, they are excellent bio sorbents. The eggshell structure is uneven and granulated. One eggshell, which consists of 95 % to 97% calcite ($CaCO_3$) crystals, contains approximately 17000 pores. The complex structure of chicken eggshell contains various organic molecules and mineralized components such as calcite (mainly in palisade and mammillary layers), which are combined in several layers. Instead of the simple $CaCO_3$ crystal layers, the shell consists of very complex mineral formations in a protein matrix. Five different organic and calcite layers build up chicken eggshell. The eggshell thickness is between 280 x 10^{-6} m and 400 x 10^{-6} m and is composed of the inner and outer membrane (70.0 x 10^{-6} m), mammillary layer (100.0 x 10^{-6} m), palisade layer (200.0 x 10^{-6} m), prismatic layer (8.0 x 10^{-6} m) and thin cuticle (10. 0 x 10^{-6} m).

Park et al. (2007) documented that several eggshells have similar or the same major chemical components. These major components include $CaCO_3$ and a few or some of these elements (namely, Si, Mg, P, S, Al, Na, Sr, K, and Sr. It was reported that eggshell contained $CaCO_3$ as limestone with a total of 97.025% and MgO with a total of 0.842%. The materials are the important inorganic compositions of eggshells.

Zhang et al. (2017), stated that the chemical components of raw or natural eggshell are Na_2O (0.492 %); MgO (0.842 %); Al_2O_3(0.054%); SiO_2(0.011%); P_2O_5(0.183%); SO_3(0.745%); $CaCO_3$ (97.025 %); K_2O (0.051%); Fe_2O_3(0.028 %); SrO (0.141%); Cl (0.127 %) and Volatile matter (0.301 %). Köse and Kivanc (2011) ; Zhang et al. (2017) reported that Brunauer, Emmett and Teller (BET), a surface area was 6.012 m^2/g; micropore volume (0.093 x 10^{-3} cm^3/g); mesopore volume (1.46 x 10^{-2} cm^3/g) and total pore volume (1.47 x 10^{-2} cm^3/g). It was stated that the natural eggshell has irregular granular crystal with 0.5 to 18 x 10^{-6} m. The comparison of the peak information of the natural eggshell implied that the main peak intensity increased; however, no aluminum hydroxide or oxide peak information was found. The reasons for this phenomenon maybe include (a) the mass of Al was too small and (b) aluminum hydroxide and oxide X-ray diffraction peak is wide. The natural eggshell exhibit one peak around 2.0 to10 x 10^{-9}m. The X-ray diffraction patterns of the natural eggshell. The main peak appeared at 2θ is equal to 29.5^o several other small peaks at 2θ equal to 23.2^o, 39.5 ^{o}, 47.3 ^{o}, 48.7 ^{o}, and 57.6 ^{o} in adsorbent. This outcome also confirms that calcium carbonate is the main constituent in the eggshell powder (Zhang et al., 2017).

Polat and Aslan (2014) stated that the key chemical compositions of by-products of eggshell are as indicated $CaCO_3$ as limestone by weight (94%), magnesium carbonate by weight is equivalent to 1% of the total weight, calcium phosphate by weight is equivalent to 1% of the total weight, and organic matter by weight is equivalent to 4% of the total weight. It was highlighted that the primary components of eggshells are in the form of $CaCO_3$ and HCO_3^-, Ca^{2+}, $CaHCO_3^+$, and $CaHO^+$. These complex ions are formed in the solution and their proportion is a function of pH or is dependent on the pH value of the medium. It was expected that any water equilibrated with the eggshell became basic confirmed with the following mechanisms (Arunlertaree et al. 2007):

$$CaCO_3 \leftrightarrow Ca^{2+} + CO_3^{2-} \quad (1)$$

$$CO_3^{2-} \leftrightarrow HCO_3^- + OH^- \quad (2)$$

As can be illustrated and seen in equation (2), the solution has become more basic due to the hydrolysis reaction of $CaCO_3$ which gives OH^- and Ca^{2+} content of the solution is also increased. In general, sorption of divalent metal cations on metal oxides, hydroxides and oxyhydroxides is known to be promoted by increasing pH. When divalent metal cations adsorb on these materials, the cations undergo a reaction with a surface hydroxyl group. Adsorption or precipitation mechanisms involve characteristic reactions of some metals with CaO and MgO surfaces, with adsorption occurring at low concentration of metals solution, and precipitation dominating at high concentrations. Carbonates formed by $CaCO_3$ dissolution increase the pH values in the solution and therefore may be formation of precipitate form of cupper precipitate near the surface of eggshell and then these forms adsorb on the eggshell.

In addition, Yusuff (2019) reported the chemical composition of eggshell as follows: Silicon oxide (SiO_2; 0.79 %); aluminium oxide (Al_2O_3 ; 0.12%); total iron oxides (Fe_2O_3 and FeO ; 2.68%); magnesium oxide (MgO, 1.78 %); Calcium oxide (CaO, 86.74%), alkali oxide

(potassium oxide, K_2O, 0.09 %); phosphate (P_2O_5; 1.21%); sulphite (SO_3 ; 0.12 %) and local organic ignition (LOI, 6.47%). Further reported in the literature such as Guru and Dash (2014) documented that eggshell is a highly well-organized structure, which comprises five structurally dissimilar layers. From the inside to the outwards, the structures include the shell membranes (inner and outer), palisade layer, mammillary layer, vertical crystal layer and cuticle. The arrangement from the inner membranes are the mineralized layer is the mammillary layer (which contain randomly orientated calcite (as $CaCO_3$) crystals). These calcite crystals layers are large with a size of greater than 1 millimetres. The palisade layer makes up the majority of the calcified portion of the shell. The palisade layer is continued as the vertical crystal layer, which is a small layer immediately underneath the cuticle. The loose and viscous–elastic porous structures provide eggshell more flexibility, and improved chemical adsorption performance. Figures 12 and 13 present scanning electron microscope and Fourier transform infrared spectra of eggshell and egg membrane. Tsai et al. (2006) reported that the results of ultimate analysis of eggshell and eggshell membrane particles revealed that the elemental contents eggshell and egg membrane are Calcium, Carbon, Hydrogen, Oxygen, Nitrogen and Sulphur. Figure 12 shows the most significant peak of intensity of eggshell particles at 1417 cm^{-1}, Which is strongly associated with the presence of carbonate minerals within the eggshell matrix (Tsai et al., 2006). There are also Mo observable peaks at about 875 cm^{-1} and 712 cm^{-1}, these two peaks should be associated with the outplane deformation and in-plane deformation modes in the presence of calcium carbonate. The EDS results revealed that powdered eggshell contains Fe, which can be in the form of Fe, Fe^{2+} or Fe^{3+}. The composition indicated that the possible redox reactions can be summarised as follows (Zubair et al., 2020):

$$Fe^{0}_{(s)} \rightarrow Fe^{2+} + 2e^{-} \quad (3)$$

$$Fe^{3+}_{(s)} \rightarrow Fe^{2+} - e^{-} \quad (4)$$

$$Fe^{2+}_{(s)}Oh + O_2(air) \rightarrow Fe^{3+}Oh \quad (5)$$

In the aqueous solution oxidative radicals (superoxide anions) could be created or generated through electron transfer from Fe component pf powdered eggshell to dissolved oxygen, as follows (Zubair et al., 2020):

$$Fe^{3+}_{(s)}Oh + e^{-} \rightarrow Fe^{2+}Oh \quad (6)$$

$$2Fe^{3+}_{(s)}Oh + As^{3+} \rightarrow 2Fe^{2+}Oh + As^{5+} \quad (7)$$

$$Fe^{2+}_{(s)}Oh + O_2(air) \rightarrow Fe^{3+}Oh + {}^{*}O_2^{-} \quad (8)$$

$$Fe^{2+}_{(s)}Oh + O_2(air) \rightarrow Fe^{3+} + {}^{*}O_2^{-} \quad (9)$$

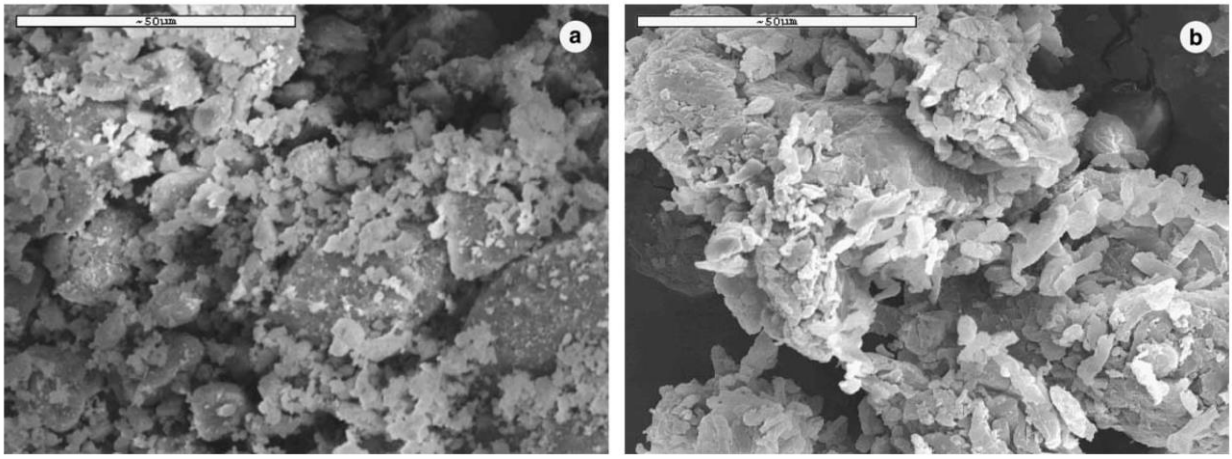

Figure 12 Scanning Electron Microscope pictures (X 1000) of eggshell, and eggshell membrane particles (Source: Tsai et al., 2006)

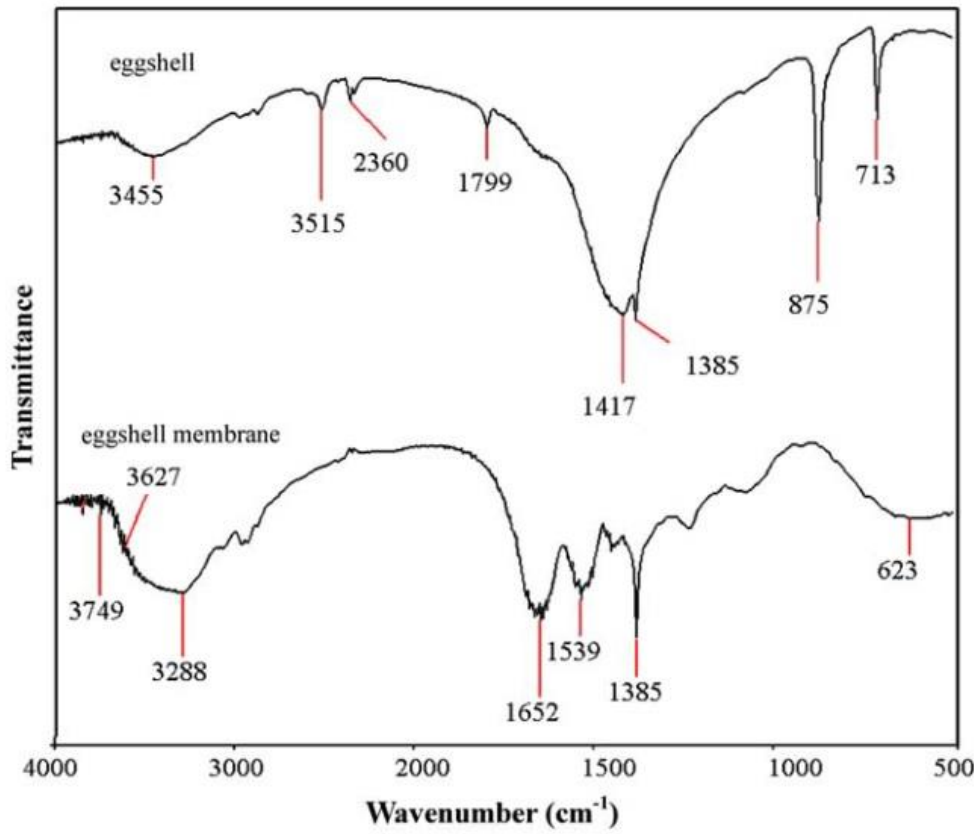

Figure 13. Fourier transform infrared spectra of eggshell and eggshell membrane particles. (Source: Tsai et al., 2006)

In conclusion, the surface redox reactions and mechanism contributed partially to arsenic reduction or removal, based on the composition of powdered eggshell cam be summarized as follows (Zubair et al., 2020):

$$Fe^{2+}_{(s)}Oh + As^{5+} \rightarrow Fe^{3+}Oh + As^{3+} \quad (10)$$

$$As^{3+} + {}^{*}O_2^{-} + 2H^{+} \rightarrow H_2O_2 + As^{4+} \quad (11)$$

$$As^{4+} + O_2 \rightarrow {}^{*}O_2^{-} + As^{5+} \quad (12)$$

$$As^{3+} + H_2O_2 \rightarrow 2OH^{-} + As^{5+} \quad (13)$$

Arsenic Adsorption Uptake Isotherm models: The adsorption equilibrium isotherm model data were fitted to three (16 isotherm models), four (4 isotherm models) and five (1 isotherm model) parameters adsorption equilibrium isotherm models. The description of these adsorption isotherm data with these twenty-one adsorption isotherm models provides insight into the relationship between the arsenic removal and the adsorbent with the adsorption type. An adsorption equilibrium model fitting with an Model Selection criterion greater than 3.00 is considered strong, which indicates possible multilayer formation and monolayer by chemical or physical adsorption. In addition, adsorbate adsorption is more favourable for multilayer adsorption than for single-layer adsorption because of the better utilization of the heterogeneous nature of the adsorbent.

The adsorption isotherm experimental data were fitted with Redlich–Peterson, Sips, Jossens, Hill, Langmuir- Freundlich, Toth, *Radke-Prausnitz,* Khan, Fritz and Schhunder, Koble – Corrigan, Liu, Weber-Van Vliet, Bauder and Marczewsk-Jaroniec models with MSC greater than 3.0 (R^2 greater than 0.971, Amoko et al., 2023) to establish the heterogeneity of the adsorption and to avoid limitations of an increase in adsorbate concentration that is associated with the Freundlich model (Amoko et al., 2023). The heterogeneity factors (γ) for arsenic removal exceeds1, which indicates that there is an heterogeneous interaction between the arsenic and the adsorbent (powdered eggshell). Figure 13 demonstrates the amount of arsenic adsorbed by powdered eggshell at equilibrium arsenic concentration for both synthetic and typical water. From the figure adsorption equilibrium and equilibrium concentrations for typical water were higher than adsorption equilibrium and equilibrium concentrations for synthetic water, which indicates more pollutants were removed in synthetic water than typical water.

These lower adsorption equilibrium and equilibrium concentrations for typical water can be attributed to the presence other pollutants. Lower adsorption performance in natural and typical surface water can be attributed to multicomponent nature of the water samples. These results and observation agreed with literature such as Cassol *et al.* (2014); Prosser and Franses (2001); Yu *et al.* (1988); Simsek and Beker (2014); Cano *et al.* (2007); Hu and Do (1995); Rudisill *et al.* (1988); Oskuli *et al.* (2019); Vilardi *et al.* (2018); Gomez-Gonzalez *et al.* (2016); Largitte and Pasquier (2016); Othman *et al.* (2019); Koopal *et al.* (2020); Hu *et al.* (2020 and 2021); Chen *et al.* (2021); Yang *et al.* (2023); Zhang *et al.* (2003); Khademi *et al.* (2018) and Thirunavukkarasu and Nithya (2020). Literature reported that the presence of other pollutants influence on As(III) adsorption onto adsorbents, which may follow the order of $H_2PO_4^-$ greater than SO_4^{2-} greater than F^- greater than HCO_3^{2-} greater than NO_3^- greater than Cl^-, and that for As(V) followed the order of $H_2PO_4^-$ greater than HCO_3^{2-} greater than F^- greater than SO_4^{2-} greater than NO_3^- greater than Cl^- .

The high adsorption capacity of the optimal adsorbents (anthill with eggshell) in the adsorption of dye from an aqueous solution may be due to the presence of the surface functional groups, among which carboxylic (C-O and C=O) and hydroxyl (OH) groups play the main role. The major compositions in the anthill sample as an adsorbent were determined to be silica (SiO_2), alumina (Al_2O_3) and zirconia (ZrO_2), while the main mineral composition in eggshells was found to be calcium oxide (CaO). The high Local Organic Ignition in the raw anthill and eggshell samples is due to the presence of organic matters and moisture content. However, CaO constitutes the larger amount in an optimal adsorbent sample, followed by SiO_2. It was observed that the calcination at 823.45 °C for 3.54 h was able to transform the mixed eggshell-anthill clay into a synergetic mixed oxide structure.

Thus, the result obtained indicates that not only CaO plays a significant role in the adsorbent performance but also the other metal oxides (SiO_2, Al_2O_3, ZrO_2 and Fe_2O_3) contained in the optimal adsorbent sample can determine the form of the molecular adsorption sites and their level of capacity. The presence of SiO_2 in the composite adsorbent plays a key role in the adsorption. SiO_2 is known as an inorganic adsorbent and could adsorb either positive or negative contaminant depending on the pH of the solution. Its surface contains silinol (-OH group), which can act as the centre of a

molecular adsorption during their specific interaction with adsorbates. Other mineral oxides, such as Al_2O_3, Fe_2O_3 and ZrO_2, also exhibit the phenomenon of electrostatic interaction. This indicates that the maximum dye adsorption capacity of the adsorbent can be attributed to the electrostatic interaction of the adsorbate with the surface CaO, SiO_2, Al_2O_3, ZrO_2 sites. This observation could be the reason that the adsorbent adsorbent had an improved performance in the adsorption of the Methly Blue dye compared to the adsorbent prepared only from eggshells, which has a single adsorption site (CaO). The results and the figure established that initial concentration of arsenic and type of aqueous solution had effect on the adsorption of arsenic

Analysis of Effects of Selected factors on Arsenic Adsorption: Tables 4 and 5 present effects of adsorption of nature of the solution on adsorption equilibrium and arsenic equilibrium concentration. These Table 4 revealed that adsorption equilibrium concentration and nature of the aqueous solution has significant effects on arsenic adsorption at a 95 % confidence level ($F_{5,5}$ = 1.476 and p- value of 0.3397 for adsorption equilibrium and $F_{1,5}$ = 16.569 with p-value of 0.010). These Table 5 revealed that arsenic equilibrium concentration and nature of the aqueous solution has significant effects on arsenic adsorption at a 95 % confidence level ($F_{5,5}$ = 2.546 and p- value of 0.1641 for adsorption equilibrium and $F_{1,5}$ = 1865.03 with p-value of 1.26 x 10^{-7}).

Performance Evaluation of Adsorption Equilibrium Models: The parameters (3, 4 and 5 parameters) obtained in fitting the field data in adsorption equilibrium were summarized in Tables 6 and 7. Figure 14 presents correlation between equilibrium concentrations and equilibrium properties for both synthetic wastewaters and typical water. It (Table 7) was clear that the adsorption data of Arsenic could be best fitted with all the adsorption equilibrium models with 4-parameters (Weber-Van Vliet, Bauder, Marczewsk- Jaroniec, and Fritz and Schhunder), 5- parameters (Fritz and Schhunder) and some of the 3 parameters (Sips, Brouers- Sotolongo, Jossens, Hill, Langmuir- Freundlich, Radke-Prausnitz, Khan, Fritz and Schhunder, Koble – Corrigan, Liu and Loading ratio) isotherm based on the values of MSC of greater than 3.0 which is greater that correlation coefficient greater than 0.95 (Amoko et al., 2023) compared with that produced by the other isotherms. Tables 6 and 7 present the detail information on these adsorption isotherms performance.

With reference to the values of MSC and AIC, it was observed the adsorption equilibrium isotherm models with MSC value greater than 3.0 are as follows: 2-parameters adsorption equilibrium isotherm models are 3 out of 17 (17.65 %); 3-parameters adsorption equilibrium isotherm models are 11 out of 16 (68.75 %); 4-parameters adsorption equilibrium isotherm models are 4 out of 4 (100 %); and 5-parameters adsorption equilibrium isotherm models are 1 out of 1 (100 %). The adsorption equilibrium isotherm models with MSC value greater than 1.0 but less than 3.0 ($3.0 < x < 1.0$) are as follows: 2-parameters adsorption equilibrium isotherm models are 6 out of 17 (35.29 %); 3-parameters adsorption equilibrium isotherm models are 1 out of 16 (6.25 %). The adsorption equilibrium isotherm models with MSC value less than 1.0 are as follows: 2-parameters adsorption equilibrium isotherm models are 8 out of 17 (47.06 %); 3-parameters adsorption equilibrium isotherm models are 4 out of 16 (25.00 %).

Table 4: Effects of arsenic adsorption equilibrium and Nature of Solution on arsenic adsorption

Source of Variation	Sum of Square	Degree of freedom	Mean Sum of Square	Statistical F-Value	Probability value	Statistical F critical at 95 % confidence level
Experiments of adsorption equilibrium	24.16338	5	4.832677	1.476454	0.339697	5.050329
Nature of Solution	54.23305	1	54.23305	16.56899	0.009629	6.607891
Error	16.36582	5	3.273165			
Total	94.76226	11				

Table 5: Effects of arsenic equilibrium concentration and Nature of Solution on arsenic adsorption

Source of Variation	*Sum of Square*	*Degree of freedom*	*Mean Sum of Square*	*Statistical F-Value*	*Probability value*	*Statistical F critical at 95 % confidence level*
Experiments of arsenic equilibrium concentration	0.04165	5	0.008329919	2.545815	0.164089	5.050329
Nature of aqueous solution	6.102373	1	6.102372773	1865.025	1.26×10^{-07}	6.607891
Error	0.01636	5	0.003272005			
Total	6.160382	11				

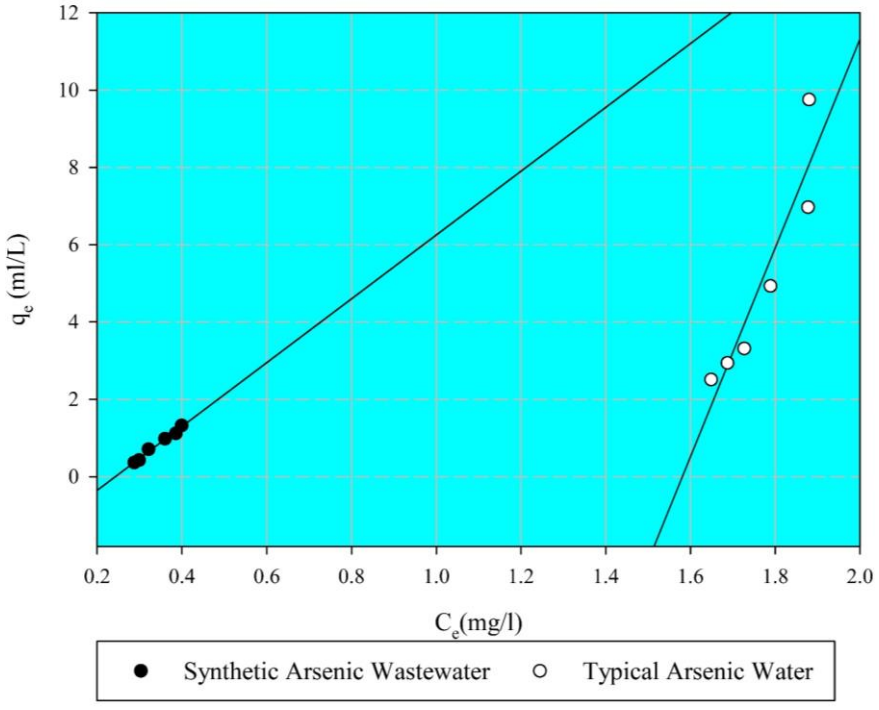

Figure 14: Correlation between adsorption equilibrium and arsenic equilibrium concentration

Table 6: the adsorption equilibrium properties and parameters of arsenic adsorption by powdered eggshell in typical water

Type	Name	Non- Linear Relationship	Parameters	K	α	β	γ	q	MSC	AIC
3- Parameters	Redlich–Peterson	$q_e = \frac{\alpha_t C_e}{1+\beta_t C_e^{\gamma}}$	α_t, γ and β_t	-	6.03 x 10^5	6.03 x 10^6	-5.89	-	1.43	15.35
	Sips	$q_e = \frac{\alpha_{ts} C_e^{\gamma ts}}{1+\beta_{ts} C_e^{\gamma ts}}$	α_{ts}, γ_{ts} and β_{ts}	-	0.034	0.0002	8.23	-	2.05	11.78
	Brouers- Sotolongo	$q_e = K_{BS}\left(1-\exp\left(-\beta_{BS} C_e^{\alpha_{BS}}\right)\right)$	$K_{BS,}$ α_{BS} and β_{BS}	3.35	2.46	3.46	-	-	-0.70	28.83
	Jossens	$C_e = \frac{q_e}{\beta_{jo}}\left(\exp\left(K_{jo} q_e^{\alpha_{jo}}\right)\right)$	α_{jo}, K_{jo}, and β_{jo},	-1.46 x 10^4	-41.68	3.52	-	-	2.194	10.94
	Hill	$q_e = \frac{K_{Hi} C_e^{\alpha_{Hi}}}{\beta_{Hi} + C_e^{\alpha_{Hi}}}$	α_{Hi}, K_{Hi}, and β_{Hi},	2.00 x 10^5	1.58	9.13 x 10^4	-	-	-0.02	24.24
	Langmuir- Freundlich	$q_e = \frac{\beta_{LF} K_{LF} C_e^{\alpha_{LF}}}{1+K_{LF} C_e^{\alpha_{LF}}}$	β_{LF}, K_{LF} and α_{LF}	0.008	7.24	14.89	-	-	0.66	20.15
	Toth	$q_e = \frac{K_{tt} \alpha_{tt}^{\gamma_{tt}} C_e}{\left(1+\alpha_{tt} C_e^{\gamma_{tt}}\right)^{\left(\frac{1}{\gamma_{tt}}\right)}}$	K_{tt}, $\alpha_{tt,}$ and γ_{tt}	11.94	1.0 x 10^{-4}	-	0.167	-	-0.14	**24.94**

Type	Name	Non- Linear Relationship	Parameters	K	α	β	γ	q	MSC	AIC
		$q_e = \frac{\alpha_{tt} C_e}{\left(\beta_{tt} + C_e^{\gamma_{tt}}\right)^{\left(\frac{1}{\gamma_{tt}}\right)}}$	α_{tt}, β_{tt} and γ_{tt}	-	4.36 x 10^4	1.30 x 10^4	0.986	-	-0.14	24.94
	Radke-Prausnitz	$\frac{1}{q_e} = \left(\frac{\alpha_{rp}}{(C_e)}\right) + \frac{\beta_{rp}}{\left(C_e^{\gamma_{rp}}\right)}$	α_{rp}, γ_{rp} and β_{rp}	-	0.001	31.30	8.66	-	3.268	-33.71
		$q_e = \frac{K_{rp}\alpha_{rp} C_e}{\left(1+\alpha_{rp} C_e^{\gamma_{tt}}\right)}$	α_{rp}, γ_{rp} and q_{rp}	1.41 x 10^{-2}	1.4 x 10^3	-	-9.46	-	1.92	12.58
	Khan	$q_e = \frac{K_k \alpha_k C_e}{\left(1+\alpha_k C_e\right)^{\gamma_k}}$	α_k, γ_k and K_k	0.003	0.131	-	-42.6	-	1.96	12.34
	Fritz and Schhunder	$q_e = \frac{K_{fs}\alpha_{fs} C_e^{\gamma_{fs}}}{\left(1+\alpha_{fs} C_e^{\gamma_{fs}}\right)}$	α_{fs}, γ_{fst} and K_{fs}	26.58	1.0 x 10^{-3}	-	12.37	-	1.97	1.23
	Frumkin	$K_{Fm} C_e = \beta_{Fm}\left(\frac{-\alpha_{Fm}\beta_{Fm}}{1-\beta_{Fm}}\right);$ $\beta_{Fm} = 1 - \frac{C_e}{C_0}$	K_{Fm}, α_{Fm} and β_{Fm}	0.208	-1.666	0.372	-	-	-2.06	31.93

Type	Name	Non- Linear Relationship	Parameters	K	α	β	γ	q	MSC	AIC
	Koble - Corrigan	$q_e = \frac{\alpha_{kc} C_e^{\gamma_{kc}}}{\left(1+\beta_{kc} C_e^{\gamma_{kc}}\right)}$	α_{kc}, β_{kc} and γ_{kc}	-	0.211	-0.072	3.69	-	2.09	11.58
	Liu	$q_e = \left(\frac{K_{li}\left(C_e\beta_{li}\right)^{\frac{1}{\alpha_{li}}}}{1+\left(C_e\beta_{li}\right)^{\frac{1}{\alpha_{li}}}}\right)$	K_{li}, β_{li} and α_{li}	558.12	10.22	0.353	-	-	2.022	11.97
	Loading ratio	$q_e = \frac{K_{Lr}\left(\beta_{Lr}C_e\right)^{\left(\frac{1}{\alpha_{Lr}}\right)}}{1+\left(\beta_{Lr}C_e\right)^{\left(\frac{1}{\alpha_{Lr}}\right)}}$	K_{Lr}, β_{Lr} and α_{Lr}	695.3	0.098	0.395	-	-	2.022	11.97
4- Parameters	Weber-Van Vliet	$C_e = K_{wvv} Q_e^{\left(\alpha_{wvv}\beta_{wvv}+\gamma_{wvv}\right)}$	K_{wvv}, α_{wvv}, β_{wvv} and γ_{wvv}	1.521	3.86	0.11	-0.33	-	8.63	-32.22
	Bauder	$q_e = \left(\frac{\left(K_{bu}\right)\beta_{bu}C_e^{1+\alpha_{bu}+\gamma_{bu}}}{1+\left(C_e^{1+\alpha_{bu}}\right)}\right)$	K_{bu}, β_{bu}, γ_{bu} and α_{bu} $1+\beta_{bu},+\alpha_{bu}<1$ And $1+\beta_{bu},<1$	8.9×10^5	10.16	9.87	0.010	-	2.02	11.961
	Marczewsk- Jaroniec	$q_e = K_{msj}\left(\frac{\left(C_e\gamma_{msj}\right)^{\alpha_{msj}}}{1+\left(C_e\gamma_{msj}\right)^{\alpha_{msj}}}\right)^{\left(\frac{\beta_{msj}}{\alpha_{msj}}\right)}$	K_{msj}, γ_{msj}, α_{msj} and β_{msj}	9.51×10^2	1.95	5.75×10^2	4.41	-	1.98	12.21
	Fritz and Schhunder	$q_e = \left(\frac{K_{FS4}\left(C_e\right)^{\alpha_{FS4}}}{1+\gamma_{FS4}\left(C_e\right)^{\beta_{FS4}}}\right)$	K_{FS4} γ_{FS4}, α_{FS4} and β_{FS4}	1.05	10.96	0.83	74.0	-	1.98	12.21
5 parameters	Fritz- Schhunder	$q_e = \left(\frac{q_{fs5}\gamma_{fs5}\left(C_e\right)^{\alpha_{fs5}}}{1+K_{fs5}\left(C_e\right)^{\beta_{fs5}}}\right)$	q_{fs5}, K_{fs5}, α_{fs5}, γ_{fs5} and β_{fs5}	4.61	10.34	0.23	0.723	0.11	2.02	11.96

Table 7: the adsorption equilibrium properties and parameters of arsenic adsorption by powdered eggshell in synthetic water

Type	Name	Non- Linear Relationship	Parameters	K	α	β	γ	q	MSC	AIC
3- Parameters	Redlich–Peterson	$q_e = \frac{\alpha_t C_e}{1+\beta_t C_e^{\gamma}}$	α_t, γ and β_t	-	2.48	0.44	20.94	-	0.35	-1.92
	Sips	$q_e = \frac{\alpha_{ts} C_e^{\gamma_{ts}}}{1+\beta_{ts} C_e^{\gamma_{ts}}}$	α_{ts}, γ_{ts} and β_{ts}	-	32.5	-0.04	3.49	-	3.24	-19.2
	Brouers- Sotolongo	$q_e = K_{BS}\left(1-\exp\left(-\beta_{BS} C_e^{\alpha_{BS}}\right)\right)$	$K_{BS,}$ α_{BS} and β_{BS}	1.50	339.97	5.659	-	-	3.66	-21.73
	Jossens	$C_e = \frac{q_e}{\beta_{jo}}\left(\exp\left(K_{jo} q_e^{\alpha_{jo}}\right)\right)$	α_{jo}, K_{jo}, and β_{jo},	-5.926	0.130	0.007	-	-	6.793	-40.56
	Hill	$q_e = \frac{K_{Hi} C_e^{\alpha_{Hi}}}{\beta_{Hi} + C_e^{\alpha_{Hi}}}$	α_{Hi}, K_{Hi}, and β_{Hi},	18.57	3.661	0.454	-	-	3.280	-19.49
	Langmuir- Freundlich	$q_e = \frac{\beta_{LF} K_{LF} C_e^{\alpha_{LF}}}{1+K_{LF} C_e^{\alpha_{LF}}}$	β_{LF}, K_{LF} and α_{LF}	1581.0	6.96	1.75	-	-	3.77	-22.4
	Toth	$q_e = \frac{K_{tt} \alpha_{tt}^{\gamma_{tt}} C_e}{\left(1+\alpha_{tt} C_e^{\gamma_{tt}}\right)^{\left(\frac{1}{\gamma_{tt}}\right)}}$	K_{tt}, $\alpha_{tt,}$ and γ_{tt}	1.48	1.05	-	10.47	-	0.35	-1.92

Type	Name	Non- Linear Relationship	Parameters	K	α	β	γ	q	MSC	AIC
		$q_e = \frac{\alpha_{tt} C_e}{\left(\beta_{tt} + C_e^{\gamma_{tt}}\right)^{\left(\frac{1}{\gamma_{tt}}\right)}}$	α_{tt}, β_{tt} and γ_{tt}	-	2.48	0.995	14.94	-	0.352	-1.92
	Radke-Prausnitz	$\frac{1}{q_e} = \left(\frac{\alpha_{rp}}{(C_e)}\right) + \frac{\beta_{rp}}{\left(C_e^{\gamma_{rp}}\right)}$	α_{rp}, γ_{rp} and β_{rp}	-	18.17	-19.47	0.916	-	3.24	-19.2
		$q_e = \frac{K_{rp}\alpha_{rp} C_e}{\left(1+\alpha_{rp} C_e^{\gamma_{tt}}\right)}$	α_{rp}, γ_{rp} and q_{rp}	32.68	1413.8	-	-2.5	-	1.06	3.09
	Khan	$q_e = \frac{K_k \alpha_k C_e}{\left(1+\alpha_k C_e\right)^{\gamma_k}}$	α_k, γ_k and K_k	0.004	7.11	-	-3.52	-	3.18	-18.9
	Fritz and Schhunder	$q_e = \frac{K_{fs}\alpha_{fs} C_e^{\gamma_{fs}}}{\left(1+\alpha_{fs} C_e^{\gamma_{fs}}\right)}$	α_{fs}, γ_{fst} and K_{fs}	15.458	2.772		3.696		3.289	-19.54
	Frumkin	$K_{Fm} C_e = \beta_{Fm}\left(\frac{-\alpha_{Fm}\beta_{Fm}}{1-\beta_{Fm}}\right);$ $\beta_{Fm} = 1 - \frac{C_e}{C_0}$	K_{Fm}, α_{Fm} and β_{Fm}	0.238	-1.331	0.236			-5.61	8.450

Type	Name	Non- Linear Relationship	Parameters	K	α	β	γ	q	MSC	AIC
	Koble - Corrigan	$q_e = \frac{\alpha_{kc} C_e^{\gamma_{kc}}}{\left(1+\beta_{kc} C_e^{\gamma_{kc}}\right)}$	α_{kc}, β_{kc} and γ_{kc}	-	2743.3	1567.9	6.95	-	3.77	-22.42
	Liu	$q_e = \left(\frac{K_{li}\left(C_e\beta_{li}\right)^{\frac{1}{\alpha_{li}}}}{1+\left(C_e\beta_{li}\right)^{\frac{1}{\alpha_{li}}}}\right)$	K_{li}, β_{li} and α_{li}	1.747	6.963	2.833	-	-	3.770	-22.42
	Loading ratio	$q_e = \frac{K_{Lr}\left(\beta_{Lr}C_e\right)^{\left(\frac{1}{\alpha_{Lr}}\right)}}{1+\left(\beta_{Lr}C_e\right)^{\left(\frac{1}{\alpha_{Lr}}\right)}}$	$K_{Lr,}$ β_{Lr} and α_{Lr}	1.75	0.144	2.88	-	-	3.77	-22.4
4- Parameters	Weber-Van Vliet	$C_e = K_{wvv} Q_e^{\left(\alpha_{wvv}\beta_{wvv}+\gamma_{wvv}\right)}$	$K_{wvv,}$ $\alpha_{wvv,}$ β_{wvv} and γ_{wvv}	0.368	4.391	0.125	-0.29	-	3.033	-23.42
	Bauder	$q_e = \left(\frac{\left(K_{bu}\right)\beta_{bu}C_e^{1+\alpha_{bu}+\gamma_{bu}}}{1+\left(C_e^{1+\alpha_{bu}}\right)}\right)$	K_{bu}, β_{bu}, γ_{bu} and α_{bu} $1+\beta_{bu},+\alpha_{bu}<1$ And $1+\beta_{bu},<1$	890178.2	2.069	9.872	8.774		4.092	-24.36
	Marczewsk- Jaroniec	$q_e = K_{msj}\left(\frac{\left(C_e\gamma_{msj}\right)^{\alpha_{msj}}}{1+\left(C_e\gamma_{msj}\right)^{\alpha_{msj}}}\right)^{\left(\frac{\beta_{msj}}{\alpha_{msj}}\right)}$	K_{msj}, γ_{msj}, α_{msj} and β_{msj}	0.528	18.5	15.91	3.52	-	4.25	-25.28
	Fritz and Schhunder	$q_e = \left(\frac{K_{FS4}\left(C_e\right)^{\alpha_{FS4}}}{1+\gamma_{FS4}\left(C_e\right)^{\beta_{FS4}}}\right)$	K_{FS4} γ_{FS4}, α_{FS4} and β_{FS4}	389.72	5.12	3.123	29.94	-	3.43	-20.36
5 parameters	Fritz- Schhunder	$q_e = \left(\frac{q_{fs5}\gamma_{fs5}\left(C_e\right)^{\alpha_{fs5}}}{1+K_{fs5}\left(C_e\right)^{\beta_{fs5}}}\right)$	q_{fs5}, K_{fs5}, α_{fs5}, γ_{fs5} and β_{fs5}	0.877	3.50	15.91	14.79	2.21	3.24	-19.24

Conclusion

With reference to the findings it can be concluded that major elemental components of the powdered eggshells are aluminium (between 1.25 and 7.58 % of the adsorbent as aluminium), Calcium (between 3.7 and 10.12% of the adsorbent as calcium), Silicon (between 11.15 and 25.62 % of the adsorbent as silicon), Carbon (between 0.00 and 27.75% of the adsorbent as carbon) and oxygen (between 48.75and 58.13% of the adsorbent as oxygen) had the highest weight percentages. There is a fair distribution of constituents of eggshell with a marked absence of several segregation in the SEM pictures. powdered eggshells removed arsenic from aqueous solutions, the removal rate was affected by the nature of the water and 5 and 4 parameters of adsorption models were effective in the description of arsenic removal by powdered eggshell. the adsorption data of Arsenic could be best fitted with all the adsorption equilibrium models with 4-parameters (Weber-Van Vliet, Bauder, Marczewsk- Jaroniec, and Fritz and Schhunder), 5- parameters (Fritz and Schhunder) and some of the 3 parameters (Sips, Brouers- Sotolongo, Jossens, Hill, Langmuir- Freundlich, Radke-Prausnitz, Khan, Fritz and Schhunder, Koble – Corrigan, Liu and Loading ratio) isotherm based on the values of MSC of greater than 3.0 which is greater that correlation coefficient greater than 0.95.

REFERENCES

Aber, S and Sheydaei, M. (2012). Removal of COD from Industrial Effluent Containing Indigo Dye Using Adsorption Method by Activated Carbon Cloth: Optimization, Kinetic, and Isotherm Studies. Clean – Soil, Air, Water., 40 (1), 87–94

Adekunbi, E. A., Babajide, J. O., Oloyede, H. O., Amoko, J. S., Obijole, O. A. and Oke I. A. (2019) Evaluation Of Microsoft Excel Solver As A Tool For Adsorption Kinetics Determination. Ife Journal of Science. 21(3), 169 – 183

Adekunbi, E.A. Obijole, O.A., Babajide, J.O. OJO, B.M., Olayanju, O.K. Bolorunduro, K.A. and Oke, I. A. (2023). Mechanism and Activation Energy of Arsenic Removal From Aqueous Solutions. Algerian Journal of Research and Technology. 7(1)46 -65. https://doi.org/10.58681.ajrt.23070106

Ajala, E.O. Eletta, O.A., Ajala, M.A. and Oyeniyi, S.K. (2018). Characterization And Evaluation Of Chicken Eggshell For Use As A Bio-Resource. Arid Zone Journal of Engineering, Technology and Environment, March, 14(1):26-40

Al-Ghouti, M.A. and Da'ana, D.A. (2020) Guidelines for the use and interpretation of adsorption isotherm models: A review, J. Hazard. Mater. 393, 122383.

Alka, S., Shahir, S., Ibrahim, N., Chai, T.-T., Mohd Bahari, Z., and Abd Manan, F. (2020). The role of plant growth promoting bacteria on arsenic removal: A review of existing perspectives. Environmental Technology and Innovation, 17, 100602. doi:10.1016/j.eti.2020.100602

Amen, R., Bashir, H., Bibi, I., Shaheen, S. M., Khan Niazi, N., Shahid, M., … Rinklebe, J. (2020). A critical review on arsenic removal from water using biochar-based sorbents: The significance of modification and redox reactions. Chemical Engineering Journal, 125195. doi:10.1016/j.cej.2020.125195

Amoko, J.S, Ojo, B.M; Babatolu, A.O; Demehin, A.I and Oke, I.A (2023). Linear And Non-Linear Of 2-Parameters Adsorption Equilibrium Isotherm Models Of Synthetic Arsenic Wastewaters. Accepted at Journal of Fundamental and Applied Agriculture

An B, Liang Q, and Zhao D (2011) Removal of arsenic(V) from spent ion exchange brine using a new class of starch-bridged magnetite nanoparticles. Water Res 2011, 45:1961–1972.

Analia I. Jose, L. M. Maja D. Marı´a, A. T. Marı´a dos S. A. and Alicia, F. C. (2019). Arsenic Adsorption on Iron-Modified Montmorillonite: Kinetic Equilibrium and Surface Complexes. Environmental Engineering Science, 37(1), 20 - 34

APHA, (2012) Standard Method for the Examination of Water and Wastewater, 22nd edn, America Water Works Association and Water Pollution Control Federation, Washington DC.

Aristizabal-Henao J, Ahmadireskety A, Griffin E, Ferreira Da Silva B and Bowden J (2020) Lipidomics and environmental toxicology: Recent trends, Current Opinion in Environmental Science and Health, 10.1016/j.coesh.2020.04.004, 15, (26-31)

Arun K, Madhavan A, Sindhu R, Emmanual S, Binod P, Pugazhendhi A, Sirohi R, Reshmy R, Awasthi M, Gnansounou E and Pandey A (2021) Probiotics and gut microbiome − Prospects and challenges in remediating heavy metal toxicity, Journal of Hazardous Materials, 10.1016/j.jhazmat.2021.126676, 420, (126676)

Arunlertaree, C., Kaewsomboon, W., Kumsopa, A., Pokethitiyook, P. and Panyawathanakit, P. Removal of lead from battery manufacturing wastewater by egg shell Songklanakarin J. Sci. Technol., 2007, 29(3) : 857-868

Aslan, S., Polat, A., and Topcu, U. S. (2015). Assessment Of The Adsorption Kinetics,

Equilibrium And Thermodynamics For The Potential Removal Of Ni^{2+} From Aqueous Solution Using Waste Eggshell. Journal Of Environmental Engineering And Landscape Management, 23(3), 221–229.

Atallah;B. Djame, N. El Hadj, M; and Samira, A. (2020). A Comparative Study of the Linear and Non-Linear Methods for Determination of the Optimum Equilibrium Isotherm for Adsorption of Pb^{2+} Ions onto Algerian Treated Clay. Iran. J. Chem. Chem. Eng. 39(4), 153 -171

Ayawei N., Newton, A E., and Wankasi, D. (2017) Review Article: Modelling and Interpretation of Adsorption Isotherms. Hindawi Journal of Chemistry. https://doi.org/10.1155/2017/3039817

Babaeivelni, K., Khodadoust, A. P., and Bogdan, D. (2014). Adsorption and removal of arsenic (V) using crystalline manganese (II,III) oxide: Kinetics, equilibrium, effect of pH and ionic strength. Journal of Environmental Science and Health, Part A, 49(13), 1462–1473.

Babajide, J.O; Adekunbi1 E. A.; Amoko, J. S; Olayanju, O.K, Bolorunduro, K.A. And **OKE, I. A** (2022). Selected operational factors effects on adsorption kinetics of Arsenic. Algerian Journal of Engineering and Research. AJER Vol 6(1), 30-43

Bailey, K. A., and Fry, R. C. (2015). *Health Effects of Prenatal and Early-Life Exposure to Arsenic. Handbook of Arsenic Toxicology, 405–428.* doi:10.1016/b978-0-12-418688-0.00017-4

Begum, S. A., Golam Hyder, A. H. M., and Vahdat, N. (2016). Adsorption isotherm and kinetic studies of As(V) removal from aqueous solution using cattle bone char. Journal of Water Supply: Research and Technology-Aqua, 65(3), 244–252.

Bentahar, Y., Hurel, C., Draoui, K., Khairoun, S., and Marmier, N. (2016). Adsorptive properties of Moroccan clays for the removal of arsenic(V) from aqueous solution. Applied Clay Science, 119, 385–392.

Calatayud M, Xiong C, Selma-Royo M and van de Wiele T (2022) Arsenolipids reduce butyrate levels and influence human gut microbiota in a donor-dependent way, Ecotoxicology and Environmental Safety, 10.1016/j.ecoenv.2022.114175, 246, (114175), Online publication date: 1-Nov-2022.

Calatayud, M., and Laparra Llopis, J. M. (2015). *Arsenic Through the Gastrointestinal Tract. Handbook of Arsenic Toxicology, 281–299.* doi:10.1016/b978-0-12-418688-0.00010-1

Candido, I. C. M., Soares, J. M. D., de Araujo Barros Barbosa, J., and de Oliveira, H. P. (2019). Adsorption and identification of traces of dyes in aqueous solutions using chemically modified eggshell membranes. Bioresource Technology Reports, 100267. doi:10.1016/j.biteb.2019.100267

Cano, T., Offringa, N., and Willson, R. C. (2007). *The effectiveness of three multi-component binding models in describing the binary competitive equilibrium adsorption of two cytochrome b5 mutants. Journal of Chromatography A, 1144(2), 197–202.*

Cassol, G. O., Gallon, R., Schwaab, M., Barbosa-Coutinho, E., Júnior, J. B. S., and Pinto, J. C. (2014). *Statistical Evaluation of Non-Linear Parameter Estimation Procedures for Adsorption Equilibrium Models. Adsorption Science and Technology, 32(4), 257–273.* doi:10.1260/0263-6174.32.4.257

Chen F, Luo Y, Li C, Wang J, Chen L, Zhong X, Zhang B, Zhu Q, Zou R, Guo X, Zhou Y and Guo L (2021) Sub-chronic low-dose arsenic in rice exposure induces gut microbiome perturbations in mice, Ecotoxicology and Environmental Safety, 10.1016/j.ecoenv.2021.112934, 227, (112934),

Chen L, Su B, Yu J, Wang J, Hu H, Ren H and Wu B (2022) Combined effects of arsenic and 2,2-dichloroacetamide on different cell populations of zebrafish liver, Science of The Total Environment, 10.1016/j.scitotenv.2022.152961, 821, (152961), Online publication date: 1-May-2022.

Chen, H. M., Liu, J., Cheng, X. Z., and Peng, Y. (2012). Adsorption for the Removal of Malachite Green by Using Eggshell Membrane in Environment Water Samples. Advanced Materials Research, 573-574, 63–67. doi:10.4028/www.scientific.net/amr.573-574.63

Cheng, X., Liu, J., Gao, Z., Pei, D., Xiong, J., and Lu, D. (2011). Adsorption Removal of Cadmium (II) from Aqueous Solution by Using Modified Eggshell Membrane. 2011 5th International Conference on Bioinformatics and Biomedical Engineering. doi:10.1109/icbbe.2011.5781612

Choi, H. (2019a). Assessment of the adsorption kinetics, equilibrium and thermodynamic for Pb(II) removal using a low cost hybrid biowaste adsorbent, eggshell/coffee ground/sericite. Water Environment Research. doi:10.1002/wer.1158

Choi, H.-J. (2019b). Assessment of the adsorption kinetics, equilibrium and thermodynamic for Pb(II) removal using a hybrid adsorbent, eggshell and sericite, in aqueous solution. Water Science and Technology. doi:10.2166/wst.2019.191

Dada, A.O, Adekola, F.A, Odebunmi, E.O, Ogunlaja, A.S. and Bello, O.S (2021). Two–three parameters isotherm modeling, kinetics with statistical validity, desorption and thermodynamic studies of adsorption of Cu(II) ions onto zerovalent iron nanoparticles.

Scientific Reports11:16454 | https://doi.org/10.1038/s41598-021-95090-8

Daus B, Wennrich R, and Weiss H: (2004). Sorption materials for arsenic removal from water: a comparative study. Water Res, 38(12):2948–2954.

Deliyanni, E. A., Kyzas, G. Z., Triantafyllidis, K. S., and Matis, K. A. (2015). Activated carbons for the removal of heavy metal ions: A systematic review of recent literature focused on lead and arsenic ions. Open Chemistry, 13(1). doi:10.1515/chem-2015-0087

Elabbas, S., Mandi, L., Berrekhis, F., Pons, M. N., Leclerc, J. P., and Ouazzani, N. (2016). Removal of Cr(III) from chrome tanning wastewater by adsorption using two natural carbonaceous materials: Eggshell and powdered marble. Journal of Environmental Management, 166, 589–595.

Elkady, M. F., Ibrahim, A. M., and El-Latif, M. M. A. (2011). Assessment of the adsorption kinetics, equilibrium and thermodynamic for the potential removal of reactive red dye using eggshell biocomposite beads. Desalination, 278(1-3), 412–423.

Fajobi, A. B.; Oke, I. A; Ojo, O. S; Bolorunduro, K. A. Olayanju, O. K. Bobola, D. G. and Oni, O. (2023) Development of Rainfall Intensity - Duration – Frequency (RIDF) Using Statistical Package for The Social Sciences (SPSS) as a Numerical Tool. LAUTECH Journal of Civil and Environmental Studies 10,(1);11 – 31. DOI: 10.36108/laujoces/3202.01.0120.

Fan, Y., Zheng, C., Liu, H., He, C., Shen, Z., and Zhang, T. C. (2020). *Effect of pH on the adsorption of arsenic(V) and antimony(V) by the black soil in three systems: Performance and mechanism. Ecotoxicology and Environmental Safety, 191, 110145.*

Feng, Q., Zhang, Z., Chen, Y., Liu, L., Zhang, Z., and Chen, C. (2013). Adsorption and Desorption Characteristics of Arsenic on Soils: Kinetics, Equilibrium, and Effect of Fe(OH)3 Colloid, H2SiO3 Colloid and Phosphate. Procedia Environmental Sciences, 18, 26–36.

Ghosh, J., and Sil, P. C. (2015). *Mechanism for Arsenic-Induced Toxic Effects. Handbook of Arsenic Toxicology, 203–231.* doi:10.1016/b978-0-12-418688-0.00008-3

Gomez-Gonzalez, R., Cerino-Córdova, F. J., Garcia-León, A. M., Soto-Regalado, E., Davila-Guzman, N. E., and Salazar-Rabago, J. J. (2016). *Lead biosorption onto coffee grounds: Comparative analysis of several optimization techniques using equilibrium adsorption models and ANN. Journal of the Taiwan Institute of Chemical Engineers, 68, 201–210.*

Guo H, Li X, Zhang Y, Li J, Yang J, Jiang H, Sun G and Huo T (2022) Metabolic characteristics related to the hazardous effects of environmental arsenic on humans: A metabolomic review, Ecotoxicology and Environmental Safety, 10.1016/j.ecoenv.2022.113459, 236, (113459),

Guru,P.S and Dash S (2014). Sorption on eggshell waste—A review on ultrastructure, biomineralization and other applications Advances in Colloid and Interface Science 209, 49–67

Hamadaoui.,Q and Naffrechoux, E (2007). Modeling of adsorption isotherms of phenol and chlorophenols onto granular activated carbon Part I. Two-parameter models and equations allowing determination of thermodynamic parameters. Journal of Hazardous Materials 147, 381–394

Hamayun, M., Mahmood, T., Naeem, A., Muska, M., Din, S. U., and Waseem, M. (2014). Equilibrium and kinetics studies of arsenate adsorption by FePO4. Chemosphere, 99, 207–215

He, X., Deng, F., Shen, T., Yang, L., Chen, D., Luo, J., … Wang, F. (2019). *Exceptional adsorption of arsenic by zirconium metal-organic frameworks: Engineering exploration and mechanism insight. Journal of Colloid and Interface Science, 539, 223–234.*

He, Z., Tian, S., and Ning, P. (2012). Adsorption of arsenate and arsenite from aqueous solutions by cerium-loaded cation exchange resin. Journal of Rare Earths, 30(6), 563–572.

Hee-Jeong C. (2019). Assessment of the adsorption kinetics, equilibrium and thermodynamic for Pb(II) removal using a hybrid adsorbent, eggshell and sericite, in aqueous solution. Water Science and Technology 79.10 1922-1933

Hee-Jeong, C. and Seung-Mok, L. (2015). Heavy metal removal from acid mine drainage by calcined eggshell and microalgae hybrid system. Environ Sci Pollut Res DOI 10.1007/s11356-015-4623-3

Hu L, Wang X, Wu D, Zhang B, Fan H, Shen F, Liao Y, Huang X and Gao G (2021) Effects of organic selenium on absorption and bioaccessibility of arsenic in radish under arsenic stress, Food Chemistry, 10.1016/j.foodchem.2020.128614, 344,

Hu, B., Cheng, Y., He, X., Wang, Z., Jiang, Z., Yi, M., … Wang, L. (2020). *Effects of equilibrium time and adsorption models on the characterization of coal pore structures based on statistical analysis of adsorption equilibrium and disequilibrium data. Fuel, 281, 118770.* doi:10.1016/j.fuel.2020.118770

Hu, Q., Liu, Y., Gu, X., and Zhao, Y. (2017). *Adsorption behavior and mechanism of different arsenic species on mesoporous MnFe 2 O 4 magnetic nanoparticles. Chemosphere, 181, 328–336.*

Hu, X., and Do, D. D. (1995). *Comparing various multicomponent adsorption equilibrium models. AIChE Journal, 41(6), 1585–1592.* doi:10.1002/aic.690410623

Jin B, Li H, Zhang H, Yang J, Ma W, L. M, Zheng X, Li X, Liu L and Wang K (2022) Effects of carnosic acid on arsenic-induced liver injury in mice: A comparative transcriptomics analysis, Journal of Trace Elements in Medicine and Biology, 10.1016/j.jtemb.2022.126953, 71, (126953), Online publication date: 1-May-2022.

Karachaliou C, Sgourou A, Kakkos S and Kalavrouziotis I (2021) Arsenic exposure promotes the emergence of cardiovascular diseases, Reviews on Environmental Health, 10.1515/reveh-2021-0004, 37:4, (467-486), Online publication date: 16-Dec-2022., Online publication date: 1-Dec-2022.

Khademi, H., Gabarrón, M., Abbaspour, A., Martínez-Martínez, S., Faz, A., and Acosta, J. A. (2019). Environmental impact assessment of industrial activities on heavy metals distribution in street dust and soil. Chemosphere 217, 695–705. doi:10.1016/j.chemosphere.2018.11.045

Khanam, R., Kumar, A., Nayak, A., Shahid, M., Tripathi, R., Vijayakumar, S.,(2019). Metal(loid)s (As, Hg, Se, Pb and Cd) in paddy soil: bioavailability and potential risk to human health. Sci. Total Environ. 699, 134330. doi:10.1016/j.scitotenv.2019.134330

Koohzad, E., Jafari, D.and EsmaeiIi H (2019). Adsorption of Lead and Arsenic tons from Aqueous Solution by Activated Carbon Prepared from Tamarix Leaves. . ChemistrySelect 2019, 4, 1 2356 – 12367. https://doi,org/10.1002/slct.201903167

Koopal, L., Tan, W., and Avena, M. (2020). *Equilibrium mono- and multicomponent adsorption models: From homogeneous ideal to heterogeneous non-ideal binding. Advances in Colloid and Interface Science, 102138.* doi:10.1016/j.cis.2020.102138

Köse, T. E., and Kıvanç, B. (2011). Adsorption of phosphate from aqueous solutions using calcined waste eggshell. Chemical Engineering Journal, 178, 34–39.

Kumar, P.R, Chaudhari, S, Khilar, K.C, and Mahajan, S. P (2004). Removal of arsenic from water by electrocoagulation. Chemosphere 55:1245–1252.

Kundu, S., and Gupta, A. K. (2006). Arsenic adsorption onto iron oxide-coated cement (IOCC): Regression analysis of equilibrium data with several isotherm models and their optimization. Chemical Engineering Journal, 122(1-2), 93–106. doi:10.1016/j.cej.2006.06.002

Largitte, L., and Pasquier, R. (2016). *New models for kinetics and equilibrium homogeneous adsorption. Chemical Engineering Research and Design, 112, 289–297.*

Li, H; Zhiwei S and Changxiong Z. (2014) Trends in Research on Electrochemical Oxidation. Croat. Chem. Acta 87 (2) 185–194

Li, Q., Xu, X., Cui, H., Pang, J., Wei, Z., Sun, Z., and Zhai, J. (2012). Comparison of two adsorbents for the removal of pentavalent arsenic from aqueous solutions. Journal of Environmental Management, 98, 98–106.

Li, R., Li, Q., Gao, S., and Shang, J. K. (2012). *Exceptional arsenic adsorption performance of hydrous cerium oxide nanoparticles: Part A. Adsorption capacity and mechanism. Chemical Engineering Journal, 185-186, 127–135.* doi:10.1016/j.cej.2012.01.061

Lin, T. F., Liu, C. C., and Hsieh, W. H. (2006). Adsorption kinetics and equilibrium of arsenic onto an iron-based adsorbent and an ion exchange resin. Water Science and Technology: Water Supply, 6(2), 201–207.

Liu X, Zhang J, Si J, Li P, Gao H, Li W and Chen Y (2023) What happens to gut microorganisms and potential repair mechanisms when meet heavy metal(loid)s, Environmental Pollution, 10.1016/j.envpol.2022.120780, 317, (120780), Online publication date: 1-Jan-2023.

López-Luna, J.; Ramírez-Montes,·L.E..; Martinez-Vargas, S. · Arturo I. M.; Mijangos-Ricardez, O. F.· María del Carmen A. González-Chávez, · R.o Carrillo-González, F. A.; Solís-Domínguez, María del Carmen, C. and · Vázquez-Hipólito, V. (2019). Linear and nonlinear kinetic and isotherm adsorption models for arsenic removal by manganese ferrite nanoparticles. SN Applied Sciences https://doi.org/10.1007/s42452-019-0977-3

Lorenzen, L., van Deventer, J. S. ., and Landi, W. . (1995). *Factors affecting the mechanism of the adsorption of arsenic species on activated carbon. Minerals Engineering, 8(4-5), 557–569.* doi:10.1016/0892-6875(95)00017-k

Malana, M. A., Qureshi, R. B., and Ashiq, M. N. (2011). *Adsorption studies of arsenic on nano aluminium doped manganese copper ferrite polymer (MA, VA, AA) composite: Kinetics and mechanism. Chemical Engineering Journal, 172(2-3), 721–727.* doi:10.1016/j.cej.2011.06.041

Manna, B., and Ghosh, U. C. (2007). Adsorption of arsenic from aqueous solution on synthetic hydrous stannic oxide. Journal of Hazardous Materials, 144(1-2), 522–531.

Matusik, J. (2014). Arsenate, orthophosphate, sulfate, and nitrate sorption equilibria and kinetics for halloysite and kaolinites with an

induced positive charge. Chemical Engineering Journal, 246, 244–253.

Min, L.-L., Yuan, Z.-H., Zhong, L.-B., Liu, Q., Wu, R.-X., and Zheng, Y.-M. (2015). Preparation of chitosan based electrospun nanofiber membrane and its adsorptive removal of arsenate from aqueous solution. Chemical Engineering Journal, 267, 132–141.

Mukhopadhyay, R., Manjaiah, K. M., Datta, S. C., Yadav, R. K., and Sarkar, B. (2017). Inorganically modified clay minerals: Preparation, characterization, and arsenic adsorption in contaminated water and soil. Applied Clay Science, 147, 1–10.

Nakano, T., Ikawa, N., and Ozimek, L. (2003). Chemical composition of chicken eggshell and shell membranes. Poultry Science, 82(3), 510–514. doi:10.1093/ps/82.3.510

Namasivayam, C., and Senthilkumar, S. (1998). Removal of Arsenic(V) from Aqueous Solution Using Industrial Solid Waste: Adsorption Rates and Equilibrium Studies. Industrial and Engineering Chemistry Research, 37(12), 4816–4822.

Obijole, O.A, Adekunbi, E. A, Babajide, O.J, Sani, B.S, Idi, M.D and OKE, I.A (2022). A Review of Techniques for Arsenic Removal From Water. Book Series Published in the United States of America by IGI Global, DOI: 10.4018/978-1-7998-7356-3.ch015

Ojo, S. O., Olayanju, O. K., Bobola, D. G.,Fajobi, A. B., Bolorunduro, K. A., Oke, I. A., and Oni, O (2023) Evaluation of Selected Computational Methods of Solving Simultaneous Equations in Environmental Science for the Treatment of Textile Wastewater. LAUTECH Journal of Civil and Environmental Studies 10,(1);32 – 46. DOI: 10.36108/laujoces/3202.01.0130

Okafor, P.C; Okon, P.U; Daniel, E.F and. Ebenso,E.E. (2012). Adsorption Capacity of Coconut (Cocos nucifera L.) Shell for Lead, Copper, Cadmium and Arsenic from Aqueous Solutions Int. J. Electrochem. Sci., 7 (2012) 12354 - 12369

Oke I. A., Fajobi A. B., Bolorunduro K. A. and Bobola, D. G.. (2022a) Modelling the Adsorption of Arsenic from Water and Wastewater using Microsoft Excel Solver. LAUTECH Journal of Civil and Environmental Studies 8,(2);83 – 93. DOI: 10.36108/laujoces/2202.80.0280

Oke I. A., Fehintola, E. O., Adekunbi, E. A. Babatolu,O.A and Demehin, A. I. (2022b). Performance Evaluation of Selected Treatment Techniques and Models of Phosphate Reduction. Science Forum Journal of Pure and Applied Sciences 22, 572 – 589

Oke, I. A.; Olarinoye, N.O. and Adewusi, S.R.A. (2008)Adsorption Kinetics for Arsenic Removal by Untreated Powdered Eggshell from Aqueous Solutions. Adsorption, 14,(1), 85-92.

Osborne, L., and Thompson, M. B. (2005). *Chemical Composition and Structure of the Eggshell of Three Oviparous Lizards. Copeia, 2005(3), 683–692.* doi:10.1643/ch-04-280r1

Oskui, F. N., Aghdasinia, H., and Sorkhabi, M. G. (2019). *Modeling and optimization of chromium adsorption onto clay using response surface methodology, artificial neural network, and equilibrium isotherm models. Environmental Progress and Sustainable Energy, e13260.* doi:10.1002/ep.13260

Othman, M. S., Sheikh Hussin, S. A., Rambli, A., and Zahid, Z. (2019). *Equilibrium Isotherm Models for the Adsorption of Methylene Blue from Wastewater. Journal of Physics: Conference Series, 1366, 012033.* doi:10.1088/1742-6596/1366/1/012033

Outram, J.G, Sara J. C., Wayde, M., and Graeme J. M.. (2021). Application of non-linear regression analysis and statistical testing to equilibrium isotherms: Building an Excel template and interpretation. Separation and Purification Technology 258, 118005

Pandi, K., Lee, D., and Choi, J. (2020). *Facile synthesis of zirconium-organic frameworks@biomass-derived porous graphitic nanocomposites: Arsenic adsorption performance and mechanism. Journal of Molecular Liquids, 113552.* doi:10.1016/j.molliq.2020.113552

Park H. J, Jeong, SW, and Yang J. K, (2007) Removal of heavy metals using waste eggshell. Journal of Environmental Sciences 19: 1436–1441.

Park, J. H., Han, Y.-S., and Ahn, J. S. (2016). *Comparison of arsenic co-precipitation and adsorption by iron minerals and the mechanism of arsenic natural attenuation in a mine stream. Water Research, 106, 295–303.*

Pierce, M. L., and Moore, C. B. (1980). Adsorption of arsenite on amorphous iron hydroxide from dilute aqueous solution. Environmental Science and Technology, 14(2), 214–216. doi:10.1021/es60162a011

Pierce, M. L., and Moore, C. B. (1982). *Adsorption of arsenite and arsenate on amorphous iron hydroxide. Water Research, 16(7), 1247–1253.* doi:10.1016/0043-1354(82)90143-9

Polat, A., and Aslan, S. (2014). Kinetic And Isotherm Study Of Cupper Adsorption From Aqueous Solution Using Waste Eggshell. Journal Of Environmental Engineering And Landscape Management, 22(2), 132–140.

Prosser, A. J., and Franses, E. I. (2001). *Adsorption and surface tension of ionic surfactants at the air–water interface: review and evaluation of equilibrium models. Colloids and Surfaces A:*

Physicochemical and Engineering Aspects, 178(1-3), 1–40. doi:10.1016/s0927-7757(00)00706-8

Ramesh, A., Hasegawa, H., Maki, T., and Ueda, K. (2007). Adsorption of inorganic and organic arsenic from aqueous solutions by polymeric Al/Fe modified montmorillonite. Separation and Purification Technology, 56(1), 90–100.

Rangabhashiyam, S. Anu, N. M.S. Giri, N. and Selvaraju, N. (2014). Review: Relevance of isotherm models in biosorption of pollutants by agricultural by-products. Journal of Environmental Chemical Engineering 2, 398–414

Rápó, E., Aradi, L. E., Szabó, Á., Posta, K., Szép, R., and Tonk, S. (2020). Adsorption of Remazol Brilliant Violet-5R Textile Dye from Aqueous Solutions by Using Eggshell Waste Biosorbent. Scientific Reports, 10(1). doi:10.1038/s41598-020-65334-0

Ro S, Bae J, Jang Y, Myers J, Chung S, Yu J, Natarajan S, Franco R and Song H (2022) Arsenic Toxicity on Metabolism and Autophagy in Adipose and Muscle Tissues, Antioxidants, 10.3390/antiox11040689, 11:4, (689)

Rudisill, E. N., and LeVan, M. D. (1988). *Multicomponent adsorption equilibrium: Henry's law limit for pore-filling models. AIChE Journal, 34(12), 2080–2082.* doi:10.1002/aic.690341220

Sahabi, D. M., Takeda, M., Suzuki, I., and Koizumi, J. (2009). Adsorption and abiotic oxidation of arsenic by aged biofilter media: Equilibrium and kinetics. Journal of Hazardous Materials, 168(2-3), 1310–1318.

Santra, D., and Sarkar, M. (2016). *Optimization of process variables and mechanism of arsenic (V) adsorption onto cellulose nanocomposite. Journal of Molecular Liquids, 224, 290–302.*

Shakoor, M.B, Nabeel, K. N., Irshad, B., Muhammad, S., Fakhra, S., Safdar, B., and Sabry, M. S. and Hailong, W., Daniel, C.W. Tsang, Y. Sik Ok, and Jörg, R. (2018). Arsenic removal by natural and chemically modified water melon rind in aqueous solutions and groundwater. Science of the Total Environment 645, 1444–1455

Sheindorf, C; Rebhun, M and Sheintuch, M. (1981). A Freundlich type Multicomponent isotherm. J. Colloid and Interface Sci. 79, 136-140

Sheindorf, C; Rebhun, M and Sheintuch, M. (1982). Organic Pollutants adsorption from mutlicomponent systems modelled by Freundlich type Isotherm. Water Research, 16, 357-362.

Shih, M.C (2005) An overview of arsenic removal by pressure-driven membrane processes. Desalination, 172(1):85–97.

Simsek, E. B., and Beker, U. (2014). *Equilibrium arsenic adsorption onto metallic oxides : Isotherm models, error analysis and removal mechanism. Korean Journal of Chemical Engineering, 31(11), 2057–2069.* doi:10.1007/s11814-014-0176-2

Singh TS, and Pant K.K (2004): Equilibrium, kinetics and thermodynamic studies for adsorption of As(III) on activated alumina. Sep Purif Technol., 36(2):139–147.

Tsai, W. T., Yang, J. M., Lai, C. W., Cheng, Y. H., Lin, C. C., and Yeh, C. W. (2006). *Characterization and adsorption properties of eggshells and eggshell membrane. Bioresource Technology, 97(3), 488–493.* doi:10.1016/j.biortech.2005.02.05

Tseng, C. H., Lee, I. H., and Chen, Y. (2019). Evaluation of hexavalent chromium concentration in water and its health risk with a system dynamics model. Sci. Total Environ. 669, 103–111. doi:10.1016/j.scitotenv.2019.03.103

Tu P, Tang Q, Mo Z, Niu H, Hu Y, Wu L, Chen Z, Wang X and Gao B (2023) Dietary Administration of Black Raspberries and Arsenic Exposure: Changes in the Gut Microbiota and Its Functional Metabolites, Metabolites, 10.3390/metabo13020207, 13:2, (207)

Valdes, S. A. C., Vieira, L. G., Ferreira, C. H., Mendonça, J. dos S., Ribeiro, P. R. Q., Fernandes, E. de A., and Santos, A. L. Q. (2015). *Effects of Exposure to Methyl Parathion on Egg Hatchability and Eggshell Chemical Composition inPodocnemis expansa(Testudines, Podocnemididae). Zoological Science, 32(2), 135–140.* doi:10.2108/zs140164

Van Loosdrecht, M.C.M., Nielsen, P.H.,Lopez-Vazquez, C.M., Brdjanovic, D., (2016). Experimental Methods in Wastewater Treatment. 1st Edition, International Water Publishing Alliance House, London

Vilardi, G., Di Palma, L., and Verdone, N. (2018). Heavy metals adsorption by banana peels micro-powder: Equilibrium modeling by non-linear models. Chinese Journal of Chemical Engineering, 26(3), 455–464. doi:10.1016/j.cjche.2017.06.026

Vishali, S. and Mullai, P. (2016): Analysis of two-parameter and three-parameter isotherms by nonlinear regression for the treatment of textile effluent using immobilized Trametes Versicolor: comparison of various error functions, Desalination and Water Treatment, DOI: 10.1080/19443994.2016.1167127

Wakeel, A., Xu, M., and Gan, Y. (2020). Chromium-induced reactive oxygen species accumulation by altering the enzymatic antioxidant system and associated cytotoxic, genotoxic, ultrastructural, and photosynthetic changes in plants. Int.J. Mol. Sci. 21, 728. doi:10.3390/ijms21030728

Wang L, Zeraatpisheh M, Wei Z and Xu M (2022), Heavy metal pollution and risk assessment of

farmland soil around abandoned domestic waste dump in Kaifeng City. Front. Environ. Sci. 10:946298. doi: 10.3389/fenvs.2022.946298

Wang, Y., Wang, S., Wang, X., Zhang, Z., and Jia, Y. (2016). *Adsorption Behavior and Removal Mechanism of Arsenic from Water by Fe(III)-Modified 13X Molecular Sieves. Water, Air, and Soil Pollution, 227(8).* doi:10.1007/s11270-016-2955-3

Wu L, Zhang S, Zhang Q, Wei S, Wang G, Luo P and Chen L (2022) The Molecular Mechanism of Hepatic Lipid Metabolism Disorder Caused by NaAsO2 through Regulating the ERK/PPAR Signaling Pathway, Oxidative Medicine and Cellular Longevity, 10.1155/2022/6405911, 2022, (1-13)

Xue X, Xiong C, Yoshinaga M, Rosen B and Zhu Y (2021) The enigma of environmental organoarsenicals: Insights and implications, Critical Reviews in Environmental Science and Technology, 10.1080/10643389.2021.1947678, 52:21, (3835-3862), Online publication date: 2-Nov-2022.

Yang Z, Zeng G, Liu L, He F, Arinzechi C, Liao Q, Yang W and Si M (2023), Simultaneous immobilization of lead, cadmium and arsenic in soil by iron- manganese modified biochar. Front. Environ. Sci. 11:1281341. doi: 10.3389/fenvs.2023.1281341

Yang, Y.; Hsiao, Y.-C.; Liu, C.-W.; Lu, K (2023). The Role of the Nuclear Receptor FXR in Arsenic-Induced Glucose Intolerance in Mice. Toxics 2023, 11, 833. https://doi.org/10.3390/toxics11100833

Yazdani, M. (Roza), Tuutijärvi, T., Bhatnagar, A., and Vahala, R. (2016). Adsorptive removal of arsenic(V) from aqueous phase by feldspars: Kinetics, mechanism, and thermodynamic aspects of adsorption. Journal of Molecular Liquids, 214, 149–156.

Yin N, Cai X, Wang P, Feng R, Du H, Fu Y, Sun G and Cui Y (2022) Predictive capabilities of in vitro colon bioaccessibility for estimating in vivo relative bioavailability of arsenic from contaminated soils: Arsenic speciation and gut microbiota considerations, Science of The Total Environment, 10.1016/j.scitotenv.2021.151804, 818, (151804),

Yin, Y., Zhou, T., Luo, H., Geng, J., Yu, W., and Jiang, Z. (2019). *Adsorption of arsenic by activated charcoal coated zirconium-manganese nanocomposite: Performance and mechanism. Colloids and Surfaces A: Physicochemical and Engineering Aspects.* doi:10.1016/j.colsurfa.2019.04.09

Yu, X., Deng, S., and Wu, P. (1988). *Evaluation of Adsorption Equilibrium Models by Means of Data Obtained for Oxygen and Nitrogen on Zeolite 5A. Adsorption Science and Technology, 5(3), 199–212.* doi:10.1177/026361748800500303

Yusuff, A. S. (2019). ADSORPTION OF CATIONIC DYE FROM AQUEOUS SOLUTION USING COMPOSITE CHICKEN EGGSHELL - ANTHILL CLAY: OPTIMIZATION OF ADSORBENT PREPARATION CONDITIONS. Acta Polytechnica, 59(2), 192–202.

Zhang, Y., Li, H., Zhang, Y., Song, F., Cao, X., Lyu, X., … Crittenden, J. (2017). Statistical optimization and batch studies on adsorption of phosphate using Al-eggshell. Adsorption Science and Technology, 36(3-4), 999–1017. doi:10.1177/0263617417740790

Zhang, Y., Yang, M., Gao, Y., Wang, F., and Huang, X. (2003). *Preparation and adsorption mechanism of rare earth-doped adsorbent for arsenic(V) removal from groundwater. Science in China Series B: Chemistry, 46(3), 252–258.* doi:10.1007/bf02883045

Zhou Y, Addai F, Zhang X, Liu Y, Wang Y, Lin F, Tuffour A, Gu J, Liu G and Shi H (2022) Heavy metal-induced lipogenic gene aberration, lipid dysregulation and obesogenic effect: a review, Environmental Chemistry Letters, 10.1007/s10311-021-01383-9, 20:3, (1611-1643), Online publication date: 1-Jun-2022.

Zhou, J., Zhou, X., Yang, K., Cao, Z., Wang, Z., Zhou, C., … Xu, X. (2019). *Adsorption behavior and mechanism of arsenic on mesoporous silica modified by iron-manganese binary oxide (FeMnOx/SBA-15) from aqueous systems. Journal of Hazardous Materials, 121229.*

Zhu, J., Lou, Z., Liu, Y., Fu, R., Baig, S. A., and Xu, X. (2015). *Adsorption behavior and removal mechanism of arsenic on graphene modified by iron–manganese binary oxide (FeMnOx/RGO) from aqueous solutions. RSC Advances, 5(83), 67951–67961.* doi:10.1039/c5ra11601e

Zhu, N., and Yan, T. (2016). *Synthesis of Manganese Chloride Activated Carbon Deriving from Wheat Straw and its Adsorption Mechanism for Arsenic and Chromium. Journal of Environmental Analytical Chemistry, 03(01).* doi:10.4172/2380-2391.1000172

Zhu, N., Qiao, J., Ye, Y., and Yan, T. (2018). *Synthesis of mesoporous bismuth-impregnated aluminum oxide for arsenic removal: Adsorption mechanism study and application to a lab-scale column. Journal of Environmental Management, 211, 73–82.*

Zhu, N., Yan, T., Qiao, J., and Cao, H. (2016). Adsorption of arsenic, phosphorus and chromium by bismuth impregnated biochar: Adsorption mechanism and depleted adsorbent

utilization. Chemosphere, 164, 32–40. doi:10.1016/j.chemosphere.2016.08.036

Zubair, Y. O., Fuchida, S., and Tokoro, C. (2020). *Insight into the Mechanism of Arsenic(III/V) Uptake on Mesoporous Zerovalent Iron–Magnetite Nanocomposites: Adsorption and Microscopic Studies. ACS Applied Materials and Interfaces.* doi:10.1021/acsami.0c14088

Abbreviations and Symbols

R is the gas constant (8.31 mol^{-1} K^{-1}); T is the absolute temperature (K); q_e is the adsorption capacity of the absorbent at equilibrium(mg/g); C_0 is the initial concentration of arsenic in the aqueous solution (mg/l); C_e is the final concentration of arsenic in the aqueous solution at equilibrium (mg/l); M is the mass of the adsorbent added (g); Γ is the Gamma function symbol; exp or Exp is the exponential and V is the volume of the water sample utilised (300ml = 0.30 litres).

k is the statistical isotherm parameter for the mass of the pollutant per unit mass of the absorbent (mg/g)

k_p is the isotherm constant for the linear model for the mass of the pollutant per unit mass of the absorbent (mg/g)

q_e is the equilibrium solid-phase concentration of sorbate t (mg/mg)

α_L and β_L are the Langmuir adsorption constant(L/mg) and Langmuir isotherm parameter (mg/g) respectively

K_f and α_f are the Freundlich isotherm exponents for pollutant mass per unit mass of the absorbent (g/mg) and Freundlich isotherm parameter for the volume of the solution per unit mass of the pollutant (L/mg) respectively

K_H and α_H are Hasley's isotherm parameters for pollutant mass per unit mass of the absorbent and for the volume of the solution per unit mass of the pollutant respectively

K_m and α_m are constant for activated sludge model as volume of the solution per unit mass of the pollutant) and exponential constant for activated sludge model as pollutant mass per unit mass of the adsorbent respectively

K_{Hr} and α_{Hr} are isotherm parameters for Halsey C (Rangabhashiyum *et al.,* 2014) as volume of the solution per unit mass of the pollutant) and exponential constant for Halsey C model as pollutant mass per unit mass of the adsorbent respectively

K_{Hf} and α_{Hf} are isotherm parameters for Halsey B (Hamdaoui and Naffrechous, 2007) as volume of the solution per unit mass of the pollutant) and exponential constant for Halsey B model as pollutant mass per unit mass of the adsorbent respectively

K_{LV} and α_{LV} are isotherm parameters for Langmur — Vageler as the volume of the solution per unit mass of the pollutant) and exponential constant for the Langmur — Vagel model as pollutant mass per unit mass of the adsorbent respectively

K_{FH} and α_{FH} are isotherm parameters for Flory — Huggins as volume of the solution per unit mass of the pollutant) and exponential constant for the Flory — Huggins model as pollutant mass per unit mass of the adsorbent respectively

K_{lk} and α_{lk} are isotherm parameters for Kiselev as volume of le solution per fruit mass of the pollutant) and exponential constant for Kiselev model as pollutant mass per unit mass of the adsorbent respectively

K_{Hd} and α_{Hd} are isotherm parameters for Hill-de Boer as volume of the solution per unit mass of the pollutant) and exponential constant for Hill-de Boer model as pollutant mass per unit mass of the adsorbent respectively

K_{FG} and α_{FG} are isotherm parameters for Folwer —Guggenhien as volume of the solution per unit mass of the pollutant) and exponential constant for Folwer —Guggenhien model as pollutant mass per unit mass of the adsorbent respectively

K_E and α_E are isotherm parameters for Elovich as the volume of the solution per unit mass of the pollutant) and exponential constant for Elovich model as pollutant mass per unit mass of the adsorbent respectively

K_{jm} and α_{jm} are isotherm parameters for Jovanovic the volume of the solution per unit mass of the pollutant) and exponential constant for Jovanovic model as pollutant mass per unit mass of the adsorbent respectively

K_{fhh} and α_{fhh} are isotherm parameters for Frenkel- Halsey- Hill the volume of the solution per unit mass of the pollutant) and exponential constant for Frenkel- Halsey- Hill model as pollutant mass per unit mass of the adsorbent respectively

K_{hj} and α_{hj} are isotherm parameters for Harkin Jura A the volume of the solution per unit mass of the pollutant) and exponential constant *for* Harkin Jura A model as pollutant mass per unit mass of the adsorbent respectively

K_{hj} and α_{hj} are isotherm parameters for Harkin Jura B the volume of the solution per unit mass of the pollutant) and exponential constant *for* Harkin Jura B model as pollutant mass per unit mass of the adsorbent respectively

K_{rw} and α_{rw} are isotherm parameters for Ruthven and Wong the volume of the solution per unit mass of the pollutant) and exponential constant for Ruthven and Wong model as pollutant mass per unit mass of the adsorbent respectively

K_{si} and α_{si} are isotherm parameters for Sheindorf et al. (1983), the volume of the solution per unit mass of the pollutant) and exponential constant for Sheindorf et al. (1983), model as pollutant mass per unit mass of the adsorbent respectively

α_{mLB} and β_{mLB} are isotherm parameters for Langmuir, Bulter and Ockrent, Schwlb, Markham and Benton, Moriguch and Kaneniwa as volume of the solution per unit mass of the pollutant) and exponential constant for Langmuir, Bulter and Ockrent, Schwlb, Markham and Benton, Moriguch and Kaneniwa model as pollutant mass per unit mass of the adsorbent respectively

β_{LF}, K_{LF} and α_{LF} are isotherm parameters for Langmuir- Freundlich isotherm exponents for the volume of the solution per unit mass of the pollutant (L/mg); the mass of the pollutant per unit mass of the absorbent (mg/g) and the mass of the pollutant per unit mass of the absorbent (mg/g), respectively

α_t,, β_t, and γ_t, are the Redlich–Peterson isotherm exponents for the volume of the solution per unit mass of the pollutant (L/mg); the mass of the pollutant per unit mass of the absorbent (mg/g) and the mass of the pollutant per unit mass of the absorbent (mg/g), respectively

α_{fs}, γ_{fst} and q_{mfs} are the Fritz and Schhunder's isotherm parameters for the volume of the solution per unit mass of the pollutant (L/mg); the mass of the pollutant per unit mass of the absorbent (mg/g) and the mass of the pollutant per unit mass of the absorbent (mg/g), respectively

α_k, γ_k and q_{mk} are the Khan's isotherm parameters for the volume of the solution per unit mass of the pollutant (L/mg); the mass of the pollutant per unit mass of the absorbent (mg/g) and the mass of the pollutant per unit mass of the absorbent (mg/g), respectively

α_{kc}, β_{kc} and γ_{kc} are the Koble-Corrigan's isotherm parameters for the volume of the solution per unit mass of the pollutant (L/mg); the mass of the pollutant per unit mass of the absorbent (mg/g) and the mass of the pollutant per unit mass of the absorbent (mg/g), respectively

α_{rp}, γ_{rp} and q_{rp} are the Radke-Prausnitz's isotherm parameters for the volume of the solution per unit mass of the pollutant (L/mg); the mass of the pollutant per unit mass of the absorbent (mg/g) and the mass of the pollutant per unit mass of the absorbent (mg/g), respectively

α_{ts}, β_{ts} and γ_{ts} are the Sips isotherm parameters for the volume of the solution per unit mass of the pollutant (L/mg); the mass of the pollutant per unit mass of the absorbent (mg/g) and the mass of the pollutant per unit mass of the absorbent (mg/g), respectively

α_{tt},, β_{tt} and γ_{tt} are the Toth isotherm parameters for the volume of the solution per unit mass of the pollutant (L/mg); the mass of the pollutant per unit mass of the absorbent (mg/g) and the mass of the pollutant per unit mass of the absorbent (mg/g), respectively

q_m, α_{tt}, and γ_{tt} are the Toth isotherm parameters for the volume of the solution per unit mass of the pollutant (L/mg); the mass of the pollutant per unit mass of the absorbent (mg/g) and the mass of the pollutant per unit mass of the absorbent (mg/g), respectively

q_m, K_{LF} and K_t are the Langmuir – Freundlich isotherm constants for the volume of the solution per unit mass of the pollutant (L/mg); the mass of the pollutant per unit mass of the absorbent (mg/g) and the mass of the pollutant per unit mass of the absorbent (mg/g), respectively

q_{mL}, b_{Ll} and k_l are the Loading ratio's isotherm parameter for the volume of the solution per unit mass of the pollutant (L/mg); the mass of the pollutant per unit mass of the absorbent (mg/g) and the mass of the pollutant per unit mass of the absorbent (mg/g), respectively

K_{md}, α_{md} and ε are the Dubinin-Radushkevich's isotherm parameters for the volume of the solution per unit mass of the pollutant (L/mg); the mass of the pollutant per unit mass of the absorbent (mg/g) and the mass of the pollutant per unit mass of the absorbent (mg/g), respectively

K_{mRu}; α_{mRu} and γ_{mRu} are the Ruthven for the volume of the solution per unit mass of the pollutant (L/mg); the mass of the pollutant per unit mass of the absorbent (mg/g) and the mass of the pollutant per unit mass of the absorbent (mg/g), respectively

α_{mLRP}, γ_{mLRP} and β_{mLRP} are the Redlich–Peterson for the volume of the solution per unit mass of the pollutant (L/mg); the mass of the pollutant per unit mass of the absorbent (mg/g) and the mass of the pollutant per unit mass of the absorbent (mg/g), respectively

α_{mFS}; β_{mFS} and γ_{mFS} are the Yon and Turnock for the volume of the solution per unit mass of the pollutant (L/mg); the mass of the pollutant per unit mass of the absorbent (mg/g) and the mass of the pollutant per unit mass of the absorbent (mg/g), respectively

α_{mFS}; β_{mFS} and γ_{mFS} are the Fritz and Schhunder for the volume of the solution per unit mass of the pollutant (L/mg); the mass of the pollutant per unit mass of the absorbent (mg/g) and the mass of the pollutant per unit mass of the absorbent (mg/g), respectively

K_{scjf}; β_{scjf} and γ_{scjf} are the Single Component Jovanovic -Freundlich for the volume of the solution per unit mass of the pollutant (L/mg); the mass of the pollutant per unit mass of the absorbent (mg/g) and the mass of the pollutant per unit mass of the absorbent (mg/g), respectively

K_{BS}, α_{BS} and β_{BS} are isotherm parameters for Brouers- Sotolongo isotherm exponents for the volume of the solution per unit mass of the pollutant (L/mg); the mass of the pollutant per unit mass of the absorbent (mg/g) and the mass of the pollutant per unit mass of the absorbent (mg/g), respectively

K_{wvv}, α_{wvv}, β_{wvv} and γ_{wvv} are isotherm parameters for Weber-Van Vliet isotherm exponents for the volume of the solution per unit mass of the pollutant (L/mg); the mass of the pollutant per unit mass of the absorbent (mg/g), exponents for the volume of the solution per unit mass of the pollutant (L/mg) and the mass of the pollutant per unit mass of the absorbent (mg/g), respectively

K_{bu}, β_{bu}, γ_{bu} and α_{bu} are isotherm parameters for Bauder isotherm exponents for the volume of the solution per unit mass of the pollutant (L/mg); the mass of the pollutant per unit mass of the absorbent (mg/g), exponents for the volume of the solution per unit mass of the pollutant (L/mg) and the mass of the pollutant per unit mass of the absorbent (mg/g), respectively

K_{msj}, γ_{msj}, α_{msj} and β_{msj} are isotherm parameters for Marczewsk- Jaroniec isotherm exponents for the volume of the solution per unit mass of the pollutant (L/mg); the mass of the pollutant per unit mass of the absorbent (mg/g), exponents for the volume of the solution per unit mass of the pollutant (L/mg) and the mass of the pollutant per unit mass of the absorbent (mg/g), respectively

K_{FS4} γ_{FS4}, α_{FS4} and β_{FS4} are isotherm parameters for Fritz- Schhunder isotherm exponents for the volume of the solution per unit mass of the pollutant (L/mg); the mass of the pollutant per unit mass of the absorbent (mg/g) and the mass of the pollutant per unit mass of the absorbent (mg/g), respectively

q_{fs5}, K_{fs5}, α_{fs5}, γ_{fs5} and β_{fs5} are isotherm parameters for Fritz- Schhunder isotherm exponents for the volume of the solution per unit mass of the pollutant (L/mg); the mass of the pollutant per unit mass of the absorbent (mg/g) and the mass of the pollutant per unit mass of the absorbent (mg/g), respectively

α_1, α_2, α_3 and q_m are isotherm parameters for Four parameters' isotherm parameter exponents for the volume of the solution per unit mass of the pollutant (L/mg); the mass of the pollutant per unit mass of the absorbent (mg/g) and the mass of the pollutant per unit mass of the absorbent (mg/g), respectively

Kmjs2; Kmjs1; β_{mjs1} and β_{mjs2} are isotherm parameters for Jain and Snoeyink exponents for the volume of the solution per unit mass of the pollutant (L/mg); the mass of the pollutant per unit mass of the absorbent (mg/g) and the mass of the pollutant per unit mass of the absorbent (mg/g), respectively

K_{mejf2}; γ_{mejf1} K_{mejf1}; β_{mejf1} γ_{mejf2} and β_{mejf2} are isotherm parameters for Extended Jovanovic -Freundlich exponents for the volume of the solution per unit mass of the pollutant (L/mg); the mass of the pollutant per unit mass of the absorbent (mg/g) and the mass of the pollutant per unit mass of the absorbent (mg/g), respectively

K_{melf2}; γ_{melf1} K_{melf1}; β_{melf1} γ_{melf2} and β_{melf2} are isotherm parameters for Extended Langmuir -Freundlich exponents for the volume of the solution per unit mass of the pollutant (L/mg); the mass of the pollutant per unit mass of the absorbent (mg/g) and the mass of the pollutant per unit mass of the absorbent (mg/g), respectively

$K_{mel2;}$ K_{mel1}; β_{mel1} and β_{mel2} are isotherm parameters for Extended Langmuir exponents for the volume of the solution per unit mass of the pollutant (L/mg); the mass of the pollutant per unit mass of the absorbent (mg/g) and the mass of the pollutant per unit mass of the absorbent (mg/g), respectively